Progress in Organic Coatings 135 (2019) 331–344

Contents lists available at ScienceDirect

Progress in Organic Coatings

journal homepage: www.elsevier.com/locate/porgcoat

Slippery paints: Eco-friendly coatings that cause ants to slip

Aurélie Féat[a,b,*], Walter Federle[c], Marleen Kamperman[b,d], Martin Murray[a], Jasper van der Gucht[b], Philip Taylor[a]

[a] AkzoNobel Decorative Paints, Wexham Road, Slough, SL2 5DS, United Kingdom
[b] Physical Chemistry and Soft Matter, Wageningen University, Stippeneng 4, 6708 WE, Wageningen, The Netherlands
[c] Department of Zoology, University of Cambridge, Cambridge, CB2 3EJ, United Kingdom
[d] Zernike Institute for Advanced Materials, University of Groningen, Nijenborgh 4, 9747 AG Groningen, The Netherlands

ARTICLE INFO

Keywords:
Ants
Attachment
Paints
Particle detachment
Slipperiness

ABSTRACT

Many insects are considered to be pests and can be serious threats to buildings. Insecticides represent an effective way to control pest insects but are harmful to the environment. As an eco-friendlier alternative, we have formulated waterborne, organic paints which provided a slippery physical barrier for leafcutter ants (*Atta cephalotes*) on vertical surfaces. Different paints were produced by varying the Pigment Volume Concentration (PVC) and amount of TiO_2 and $CaCO_3$ particles, and characterised in terms of contact angles, surface roughness and scrub resistance. The paints' slipperiness for *A. cephalotes* ants was evaluated in climbing tests on vertical paint panels (by recording the percentage of fallen ants). Two main factors reduced the insects' attachment to vertical paint surfaces: (1) the PVC: in paints above a critical PVC, more loose particles detach from the coating and thereby reduce insect attachment; and (2) the type, dimensions and shape of solid particles: $CaCO_3$ particles detach more easily from the paint than TiO_2, probably due to their larger size and platelet shape. Paints formulated at PVC 70 and containing 20 wt% $CaCO_3$ showed the best performance in terms of slipperiness, as well as providing good scrub resistance.

1. Introduction

1.1. Motivation and existing methods to tackle insect pests

Many insects are considered pests, because they pose serious threat to agriculture, forestry, buildings and human health (see e.g. [1–3]). Many crawling insects, most notably termites, cockroaches and ants, cause damages to buildings and furniture, or can affect hygiene and human health [4,5]. About 2300 termite species have been discovered, of which 183 species were accounted for damaged buildings as they feed primarily on wood, mostly in Asia, Australia, Africa and in the USA, causing annual damages between $2 and $40 billion [6–8]. Many cockroach species are significant indoor pests worldwide, and can increase domestic exposure to allergens associated with asthma [5]. About 0.5% of ant species are considered pests, such as fire ants and Pharaoh ants, and have been acknowledged to be the most difficult pests to eliminate [4,9,10]. Ants enter buildings in search of food or cause structural damage as they establish their nests close to heat sources, especially in cooler climates [9,10]. Thus, it is essential to prevent pest insects from entering buildings. Existing methods to do so will be briefly reviewed in this section.

Chemical treatments are widely used to tackle insect pests and include insecticide sprays, groomable coatings, baits, soil termiticide injection, and chemical fumigation [4,10,11]. These methods rely on insecticides, which are an effective way to control pests but cause environmental and health damage. In the United States only, the impact of pesticides (including insecticides) on health and environment were estimated in 2005 to cost more than $8 billion annually [12], and the serious worldwide decline of insects may be partly based on the widespread use of insecticides [13].

Physical barriers can be used to prevent crawling insects from entering buildings [11]. They rely on concrete slabs, graded particles with specific sizes or sheets made of metal or plastic, and are non-toxic [14,15]. However, such barriers do not protect buildings from drywood termites [15]. Other physical methods of combatting pest insects include heat, freezing, electricity, and microwaves, but are impractical to use in large areas [11].

Slippery paints and coatings may provide superior alternatives to the above methods as they are easy to apply, cheap, and durable, and combine aesthetic appearance with insect-repellent properties [16]. Using environmentally-friendly essential oils and plant extracts in paint coatings is an effective alternative way to repel insects from buildings

* Corresponding author.
E-mail address: aurelie.feat@akzonobel.com (A. Féat).

https://doi.org/10.1016/j.porgcoat.2019.06.004
Received 13 March 2019; Received in revised form 31 May 2019; Accepted 2 June 2019

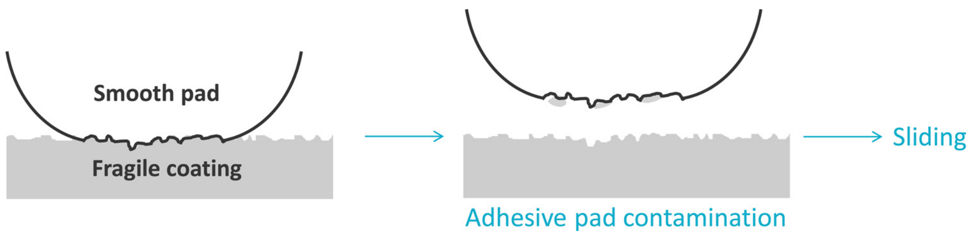

Fig. 1. Schematic showing the contamination mechanism of smooth adhesive pads on slippery, fragile surfaces.

[17]. The efficacy of such coatings, however, needs to be improved, as essential oils have been reported to repel insects for only up to a few hours [11,18], and can be increased to up to one year once incorporated into coatings [19]. Nanoparticles such as calcium carbonate and diatomaceous earths, both of which are commonly found in paints, showed insecticidal activity as insects die by desiccation after contact with these abrasive particles [20–22]. The commonly used titanium dioxide particles are genotoxic to some insect species [23]. Dispersions made of calcium carbonate particles in gelatine were also found to prevent wood infestation by termites for two years, and up to five years when combined with zinc oxide particles [24], but such dispersions cannot be readily used as exterior coatings as they would not resist e.g. weathering.

Both ants and termites are of high ecological importance as many species increase soil quality and aeration [25–28], an eco-friendlier alternative strategy to toxic insecticides is to develop coatings that prevent crawling insects from adhering to the surface by making it slippery. To this end, understanding insect locomotion and how to reduce their attachment to surfaces is of major importance.

1.2. Insect locomotion on surfaces

In nature, insects climb plant surfaces by sickle-shaped claws and adhesive pads that release an adhesion-mediating fluid [29–32]. Insect adhesive pads can conform to surface asperities, thereby increasing adhesion on rough substrates [32,33]. Two categories of adhesive pads can be found in different insect orders: smooth and hairy pads [29,34,35]. Both types of pad secrete fluids, which can fill out surface irregularities, and thereby increase the contact area and adhesion to rough surfaces [36–38]. Fluid-mediated wet adhesion in insects occurs through van der Waals, capillary and viscous forces (Stefan adhesion) [30,39,40]. Second, the claws enable the insects to interlock with the substrate's protrusions [41,42].

The oily phase of the adhesive secretion allows insects to adhere to a wide variety of substrates [29,43,44]. The effect of surface chemistry or surface hydrophobicity on fluid-mediated insect attachment has been studied on both natural and synthetic surfaces, and only weak or no effects were observed [45–47]. Substrate roughness has been found to dominate insect attachment forces over surface chemistry [46–48]. One interesting exception where surface chemistry plays an important role is the underwater attachment of dock beetles *Gastrophysa viridula* De Geer (Coleoptera, Chrysomelidae); here, adhesion forces were strongly reduced on hydrophilic substrates [49].

The effect of surface roughness on insect attachment has been investigated in many studies on hairy and smooth pads. It was shown that insects produce stronger attachment forces both on 'smooth' and coarse 'rough' substrates, but their attachment is reduced on micro-rough surfaces (0.05-1 μm asperity size) [30,46,50–53]. The function of micro-rough surfaces in reducing insect attachment is explained by its effect on both claws and adhesive pads. The roughness of these surfaces reduces the contact area for adhesive pads, but the asperities are too small to allow interlocking of the claws [50,51,53].

Inspiration from nature can improve the functionality of coatings, as demonstrated by the well-known example of self-cleaning paints inspired by the surface of lotus leaves (*Nelumbo nucifera*, Gaertn., Nelumbonaceae) [54,55]. The superhydrophobicity of lotus leaves mediated by hierarchically arranged surface structures causes water to roll off the surface and wash away particles [54]. This so-called Lotus-effect has given rise to extensive research in anti-adhesive, self-cleaning coatings, such as the exterior Lotusan paint [55].

In nature, many plant surfaces are known to be slippery to insects, in particular insect-trapping surfaces of plants covered with nano- to micrometre-sized epicuticular wax crystals, such as those found in *Nepenthes* pitcher plants, which mostly feed on ants as they fall in their traps [30,56–59]. Both the small size and likely brittleness of wax crystals reduce their suitability for the interlocking of insect claws, and the surfaces they form are too rough for insect adhesive pads to develop sufficient contact area [50,53,60,61]. Most epicuticular wax crystals also break off easily under mechanical load, leading to pad contamination, and a loss of adhesion [56,61] (Fig. 1).

From a biological and biomimetic perspective, it is of interest to understand to what extent (1) particle detachment, (2) surface roughness and (3) surface lubrication contribute to reducing insect attachment on surfaces [62]. The bioinspired, slippery SLIPS surfaces developed by Aizenberg and co-workers combine surface roughness, lubrication and porosity [63–65]. The perfluorinated lubricants, however, are harmful to the environment and deplete after a certain number of uses [66]. Eco-friendlier, non-fluorinated and more durable lubricant solutions are hence being investigated [66,67].

Zhou et al. studied insect attachment on various micro-structured substrates produced by photolithography and nanoimprinting with different pillar spacings (3-22 μm) and heights (0.5 and 1.4 μm) [68]. Adhesive pads on the feet of cockroaches (*Nauphoeta cinereal* Olivier (Blattodea, Blaberidae) smooth pads) and dock beetles (*G. viridula*, hairy pads) were found to make only partial contact on dense arrays of micropillars, whereas full contact was observed for wider pillar spacing ($>$ 4 μm) and shorter pillars (0.5 μm).

The recent work of Graf et al. [69] achieved some reduction of insect attachment to polymer films with a dual-scale rough surface, where the larger-scale asperities had a spacing of 2 μm and asperity height of 0.9 μm. In containers covered with the polymer film, the escape rate of cockroaches (*N. cinerea*, smooth pads) was reduced by 44%, but no effect was found for beetles (*G. viridula*, hairy pads) [69]. These results suggest that surfaces can be selective for particular insects, which would have potential applications, such as allowing access to beneficial insects but not pest insect species. However, the result may also be explained by the fact that *N. cinerea* cockroaches are generally 'poorer' climbers than *G. viridula* beetles on various surfaces, including polymer films [69,70].

In insect rearings, waterborne polytetrafluoroethylene dispersions (PTFE, Fluon or Teflon) are used to prevent insects from escaping their cages [71,72]. Fluon-coated walls are very slippery to insects, as aggregates of PTFE particles detach from the surfaces and adhere to their pads (Fig. 2). However, climbing ants can remove Fluon coatings from the walls of their nest containers (A.F. & W.F., personal observation), and the coatings are significantly less slippery under high humidity conditions [28].

1.3. Formulation of paints slippery to ants

As an eco-friendlier alternative to insecticidal coatings, we have formulated model waterborne, organic paints which provide a slippery

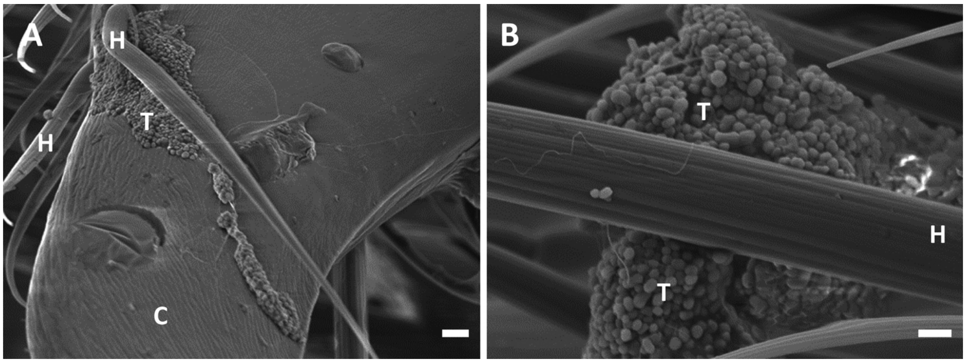

Fig. 2. SEM images from *Atta cephalotes* tarsi after walking on a wall painted with Fluon coating (Blades Biological Ltd, Edenbridge, UK). Fluon is a slippery coating used to retain insects in their nest containers. Some areas of (A) claws and (B) tarsus' hairs are covered in PTFE particles. Labels: H: hairs, T: PTFE, C: claw. Scale bars: 1 μm.

physical barrier for crawling insects on vertical surfaces. The different paint components were systematically varied to investigate the effect of wettability, surface roughness and scrub resistance, and their slipperiness for *Atta cephalotes* L. ant workers (Hymenoptera, Formicidae) using climbing tests. The working principle of the inner wall of pitcher plant traps, causing insects to slip on a surface covered by wax crystals, inspired the paint components used in this study.

Paints are made of four major ingredients: (1) the solvent, most often water for improved health and environmental impact [73,74]; (2) the pigment which brings opacity to the coating, e.g. TiO_2; (3) the polymer binder, or latex, which wets the solid particles and forms a film *via* coalescence once applied to a substrate [75,76]; and (4), the additives, such as dispersing and biocide agents [77]. Although the monomers used in the present study are typically found in market-available coatings, our organic paints represent an eco-friendlier insect-repellent alternative owing to the absence of volatile insecticide. One of the key paint formulation parameters is the Pigment Volume Concentration (PVC), which refers to the volume of pigment with regard to the volume of binder [78,79]:

$$PVC = \frac{Volume\ of\ pigments}{Volume\ of\ pigments + volume\ of\ binder} \quad (1)$$

Above a threshold value stated as the Critical Pigment Volume Concentration (CPVC), there is not enough binder to wet the pigment particles, leading to a dramatic decrease of most paint properties (e.g. gloss, durability), as well as a fragile and non-coherent coating. The CPVC of a pigment-binder system is affected by many parameters. The CPVC was found to depend on the functional monomers used and size of the polymer binder [80,81]. The presence of certain additives such as thickeners can contribute to binding as well. The CPVC is also lower for waterborne polymers than for their solventborne counterparts [81].

2. Materials and methods

2.1. Materials

Methyl methacrylate (MMA), butyl acrylate (BA), acrylic acid (AA), sodium bicarbonate, *tert*-Butyl hydroperoxide (*t*-BHP), sodium persulfate (NaPS), sodium dodecylbenzenesulfonate and AMP 95 were obtained from Sigma-Aldrich (Gillingham, UK) and used as received. Sodium dodecyl sulphate (SDS, CMC = 7.9 mM, surface tension measurement) was used both as a stabiliser in the latex synthesis and a dispersant in the paints and was supplied by VWR (Lutterworth, UK). Bruggolite FF6 was purchased from Brueggemann (Heilbronn, Germany). Texanol was added as a coalescent and was bought from Eastman (Kingsport, TN, USA). The titanium dioxide pigment used, Tiona 595, was supplied by Cristal (Grimsby, UK) and is an aluminate- and zirconia-coated rutile with a density of 4.1 g/cm^3 and a mean particle size of 300 nm (Fig. 3A). The extender was a ground calcium carbonate from Omya (Orgon, France), Omyacoat 850-OG, with a density of 2.7 g/cm^3 and a mean particle size of 1 μm (Fig. 3B).

In the present work, the number of ingredients was restricted as much as possible to limit the number of possible interactions between the paint components. The model paint systems were therefore composed of only latex (polymer binder), dispersant, pigment, extender and coalescing agent and did not contain supplementary additives found in paints, such as anti-foaming agents, thickeners or biocides.

2.2. Latex synthesis and characterisation

Latexes, or polymer binders, are one of the main ingredients in paints, as the paint coating is formed *via* coalescence and evaporation of water. Since they bind the solid particles together, their physical properties are of major importance to understand the paint coating's properties. Acrylic binders are widely used in the coating industry given their dirt pick-up resistance, durability, UV stability, etc. [74].

An approximately 40 wt% poly(methyl methacrylate-*co*-butyl acrylate-*co*-acrylic acid) (P(MMA/BA/AA)) (52/45/3) latex was prepared by seeded semi-batch emulsion polymerisation following a conventional procedure, see e.g. [74,81,82]. These monomers are typically found in binders used in the coating industry. SDS, sodium bicarbonate and demineralised water were first pre-heated in a 1L-reactor to 70 °C and stirred at 200 rpm. The seed was composed of 10 wt% of total monomers and 20 wt% of total initiator (sodium persulfate (NaPS)) and was prepared by batch emulsion polymerisation after adding them to the reactor. The remaining monomers and initiator (feed) were then added over the course of three hours at 75 °C to grow the latex particles (Table 1). After cooling to 70 °C and 60 °C, 0.05 wt% *t*-BHP and 0.05 wt % Bruggolite FF6 were respectively injected to react with the potentially remaining unreacted monomers and reduce the Volatile Organic Components (VOC) [83]. The latex was filtered after being cooled down to 30 °C.

The physical properties of the P(MMA/BA/AA) latex are shown in Table 2. The particle size was determined by Dynamic Light Scattering (Delsa Nano C from Beckman Coulter, Brea, CA, USA) and was about 70 nm (68 nm ± 1 nm, $n = 10$). The 41.9% ± 1.0% ($n = 3$) solids content was measured by gravimetric analysis. To measure the molecular weight (M_w) via Gel Permeation Chromatography (GPC), the latex was first diluted in 4% acetic acid in tetrahydrofuran (THF) and filtered through a 0.2 μm PTFE membrane. The results were relative to a polystyrene calibration over the molecular weight range 580–8500000 g/mol (Viscotek TDA 305, Malvern, Worcestershire, UK).

The glass transition temperature (T_g) of the latex was determined to be 28.0 °C ± 0.8 °C ($n = 3$), which was obtained by Differential Scanning Calorimetry (DSC, Q2000, TA Instruments, Elstree, UK), after drying the latex for 24 h at room temperature. The minimum film formation temperature (MFFT) was measured using a temperature bar (Rhopoint MFFT, Bexhill, UK) and corresponds to the lowest temperature at which a clear and coherent latex film is formed, which was 13.0 °C ± 0.6 °C ($n = 3$). 100 μm latex films were applied to glass panels using a film applicator (TQC Sheen, Rotterdam, The Netherlands) and dried for 24 h. The dry latex film showed high wettability, with a

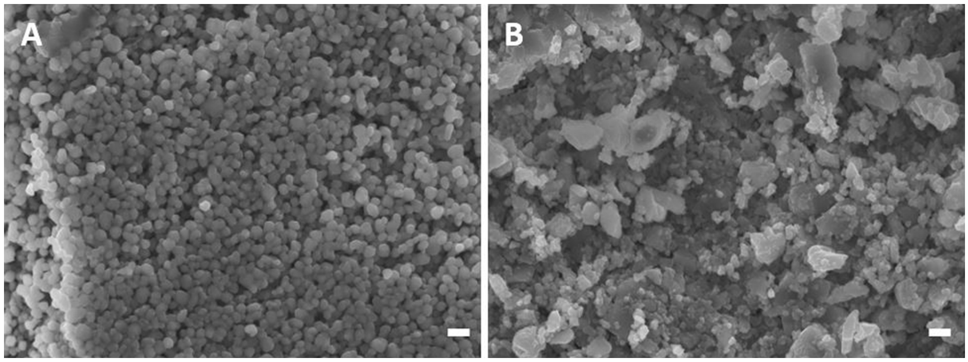

Fig. 3. SEM images of the (A) titanium dioxide (Tiona 595, spherical shape, mean diameter: 300 nm) and (b) calcium carbonate (Omyacoat 850-OG, platelet shape, mean diameter: 1 μm) grades used in this study. Scale bars: 1 μm.

Table 1
Formulation of the poly(methyl methacrylate-*co*-butyl acrylate-*co*-acrylic acid) latex used in this study. In short, it was prepared by emulsion polymerisation by feeding monomers (MMA, BA and AA) and initiator at 75 °C to a pre-emulsion (seed) made of monomers stabilised by SDS. *t*-BHP and Bruggolite FF6 were added once the feed was complete to react with potentially unreacted monomers. The final latex was obtained after filtering it at 30 °C.

Ingredient	Function	Initial volume (g)	Seed (g)	Feed (g)	Reducing feed (g)
Water	Solvent	464.9	20.0	80.0	16.7
SDS	Surfactant	11.8			
$NaHCO_3$	pH buffer	2.5			
MMA	Monomer		20.8	187.2	
BA	Monomer		18.0	162.0	
AA	Monomer		1.20	10.8	
NaPS	Initiator		0.60	2.40	
t-BHP	Initiator				0.50
Bruggolite FF6	Reducing agent				0.50

water contact angle of 26.8° ± 1.6° (n = 4).

2.3. Waterborne model paint systems and characterisation

2.3.1. Paint preparation

45 waterborne paints were prepared as follows: 70 wt% TiO_2 and 75 wt% $CaCO_3$ slurries were prepared by dispersing the solids in water at about 2000 rpm using a Dispermat high speed disperser blade (VMA–Getzmann, Reichshof, Germany) with 0.4 wt% and 0.3 wt% SDS, respectively. The optimum amount of surfactant was determined by the minimum viscosity dispersant demand method [84,85]. Various TiO_2 and $CaCO_3$ quantities (0, 10, 20, 30 wt% and 0, 6.6, 13, 20 wt%, respectively) were combined at three different PVCs (50, 60 and 70) by adding the corresponding amount of neutralised latex.

These pigment and extender quantities are typically found in high PVC commercial paints. 3 wt% Texanol, based on the total formulation, was added to each paint formulation to aid the latex coalescence process and limit the formation of cracks.

The pH of the paints was brought to 8–8.5 by adding, if necessary, AMP 95. These pH values are typically used in the coating industry, as (1) the effect of Texanol has been found to be optimised at alkaline pH [86] and (2) ensures that the anionic surfactants that stabilise the latexes and pigments are fully ionised.

2.3.2. Paint characterisation

The paints were applied on metal panels (10.5 cm × 8.5 cm) using a square film applicator (TQC Sheen, Rotterdam, The Netherlands) with a wet thickness of 100 μm and dried 24 h at 21.5 ± 0.4 °C and 49 ± 1.9%RH. The panels were 0.15 mm thick steel sheets from Ernst Sauter AG (Reinach, Switzerland) and possessed a surface roughness of 0.9 μm ± 0.2 μm.

Contact angle measurements were performed with an OCA 50 from DataPhysics (Filderstadt, Germany) using 5 μL droplets of Milli-Q water at 20.5 ± 0.5 °C and 38 ± 2.0%RH. Four measurements were carried out at different locations on the panel.

The surface roughness of paint coatings was measured using NanoFocus µScan Explorer (Oberhausen, Germany). Six measurements of 1 mm × 1 mm area (500 nm XY-resolution, 15 nm Z-resolution, 1001 pixels × 1001 pixels) were performed on the panels. The average roughness (R_a) profiles were analysed with µsoft analysis. A 'peak' was defined as any protruding region larger than 5% of the highest asperity relative to the midline, enabling access to the maximum peak height and peak density from the roughness profiles.

Scanning electron microscopy (SEM) images were obtained with JSM7001 F from JEOL (Tokyo, Japan) by prior sample coating with a 30-nm carbon layer using Q150 T ES (Quorum Technologies, Laughton, UK). The images were recorded at an acceleration voltage of 10.0 kV.

The scrub resistance of PVC 70 coatings was determined by abrasion weight loss tests according to the ASTM D4213-96 standard method. The paints (wet thickness = 400 μm) were applied to PVC scrub panels and dried for 7 days at 40 °C ± 1 °C. The coated panels were then scrubbed to either 200 or 2000 cycles at a speed of 36 cycles/min with a nylon-silicon carbide abrasive pad (40 mm × 94 mm, R_a = 30.0 ± 16.9 μm, Scotch-Brite, 3 M, St. Paul, MN, USA). A force of 2.4 N was applied onto the pads in a surfactant-based scrub medium (2.5 g/L sodium dodecylbenzenesulfonate). The scrub resistance is measured as follows:

$$Scrub\ resistance\ (mg.\ cm^{-2}) = \frac{weight\ loss}{scrubbed\ area} \quad (2)$$

Table 2
Physical properties of the P(MMA/BA/AA) latex used in this study. M_w, T_g and MFFT refer to the polymer's molecular weight, glass transition temperature and minimum film formation temperature, respectively. The solid content and M_w were measured on samples of wet latex, while temperature transitions were measured on dried samples of polymer. The water contact angle was measured on a glass panel coated with polymer. The values are expressed as mean ± standard deviation (SD).

Particle size (nm)	Solid content (%)	M_w (kDa)	T_g (°C)	MFFT (°C)	Water contact angle (°)
68 ± 1 (n = 10)	41.9 ± 1.0 (n = 3)	633 (n = 1)	28.0 ± 0.8 (n = 3)	13.0 ± 0.6 (n = 3)	26.8 ± 1.6 (n = 4)

When PVC > CPVC, there is not enough binder to fully wet the pigment particles, leading to a dramatic decrease of most paint properties (e.g. gloss, durability). The approximate CPVC values of the paint systems were between 54–63% as calculated using the oil absorptions provided by the suppliers (Table S 1, Supplementary material) [78]:

$$CPVC\,(\%) = \frac{100}{1 + \frac{pigment\ density \times oil\ absorption}{linseed\ oil\ density}} \quad (3)$$

with linseed oil density $= 0.93\,kg/L$. In the coating industry, the oil absorption of binders is estimated from the required amount of linseed oil to saturate 100 g of pigment or extender (volume of linseed oil adsorbed per unit volume of pigment) [78]. As it reflects how much binder will be needed to fully wet the solid particles, high PVC coatings containing particles with high oil absorption values are likely to be mechanically fragile.

2.3.3. Insect climbing experiments

In order to select model climbing insects, we conducted preliminary tests on paint substrates on several insect species with smooth pads (weaver ants, *Oecophylla smaragdina* Fab., Hymenoptera, Formicidae); leaf cutting ants, *A. cephalotes*; stick insects, *Carausius morosus*, Sinéty; Phasmatodea, Phasmatidae; and cockroaches, *N. cinerea*), as well as hairy pads (flies, *Calliphora vicina* Robineau-Desvoidy, Diptera, Calliphoridae; and dock beetles, *G. viridula*) [70]. While there are differences in adhesive forces between different insect species, the performance of both types of pad is very similar [36], and substrates slippery for one type are also slippery for the other [70,87]. As leaf cutting ants (*A. cephalotes*) are motivated climbers, we selected them for the climbing experiments as representatives of insects with smooth adhesive pads. Adult workers were taken from a large, 5-year-old laboratory colony kept at 24 °C and fed on bramble leaves.

The ant workers first had their pads cleaned by allowing them to walk on soft tissue paper (Tork, Dunstable, UK) and were then placed on a paint-free starting platform (1 cm^2 of 201E masking tape, 3 M, St. Paul, MN, USA) located in the middle of the vertically oriented paint panel (100 μm thickness). Once 4 (out of 6) legs had left the starting platform, the time needed to reach the edge of the paint panel was measured. The test was discarded if the insect slipped from the surface within less than three seconds after placing it on the starting platform. The insect was considered "unsuccessful" if it slipped or did not reach the edge of the panel within two minutes. Ants that reached the edge of the paint panel by walking were considered "successful". Ten ants were tested on each paint panel; each ant was not used more than three times per day to avoid any adaptive or learning effects [88].

The paint slipperiness was calculated as follows:

$$Paint\ slipperiness\ (\%) = \frac{100 \times number\ of\ unsuccessful\ ants}{number\ of\ tested\ ants} \quad (4)$$

A video of a climbing test is given in the Supplementary material. Non-painted, smooth metal sheets were used as controls; all ants could climb up these surfaces without any difficulty.

To assess the long-term durability of the paint and its slipperiness following intense exposure to ants attempting to climb on them (termed here 'long-term slipperiness'), paint panels were placed vertically on the walls inside the ants' nest container and were left there for five months. The slipperiness of these panels was measured approximately bimonthly, by the proportion of unsuccessful ants. Ants which walked on the panel for less than three seconds were discarded from the test.

To observe ant adhesive pads (referred to as arolia) under the SEM, samples were prepared as follows: immediately after climbing on paint surfaces, the ant's legs were cut off and mounted on SEM stubs using conductive carbon double-sided adhesive taSpe. The samples were frozen for 48 h to limit arolium deflation and facilitate the observation of particles [89]. Samples were then coated with a 30-nm carbon layer. Control ant samples which had not climbed the paints were observed under SEM to verify that the contaminants present on pads only came from the coatings. Images were recorded at an acceleration voltage of 5.0 kV. ImageJ (Version 1.51 r, National Institutes of Health, Bethesda, MD, USA) was used to measure the claw tip radius and the spacing between the two claws from the micrographs.

2.4. Statistics

When values with distributions are given in the text, they are expressed as mean ± standard deviation (SD). All data were tested for normal distribution. Mann–Whitney tests (*U*-tests) were used for non-normally distributed unpaired data; paired and independent *t*-tests were used otherwise. All the performed tests were two-tailed; *P*-values below $\alpha = 0.05$ were interpreted as significant differences. Multi-way ANOVA (type II) and Principal Component Regression (PCR) analyses were performed was performed using R v3.4.4 (Vienna, Austria) [90]. Since the slipperiness data were not normally distributed, they were arcsine-transformed to achieve a homogeneous distribution of the variances of the residuals resulting from ANOVA analysis. Student's *t*-tests were carried out in Microsoft Excel 2016 (Microsoft Office, Redmond, WA, USA). Mann-Whitney *U*-tests and Spearman's rank test were done using Social Science Statistics (https://www.socscistatistics.com).

3. Results and discussion

3.1. Latex and paint characterisation

To study the effect of the paint composition on leafcutter ant attachment, we investigated the systematic variation of the amount of TiO_2 and $CaCO_3$, as described in the Materials and methods section, hereby modifying the PVC values.

Paints were formulated at three different PVC values, 50%, 60% and 70%, by varying the amount of pigment and extender with regards to the quantity of latex. At PVCs 60 and 70, the paints were above their CPVC (ca. 55%), so that there was not enough binder to completely wet the particles (Fig. 4). One can see that paints formulated above their CPVC (Fig. 4B and C) lack polymer to bind efficiently all particles and tend to be porous [80,91].

The pigment and the extender present different sizes and shapes: the TiO_2 spherical particles have a diameter of about 300 nm (280 ± 60 nm, $n = 39$), while the $CaCO_3$ particles are platelet-shaped and about 1 μm in length (941 nm ± 156 nm, $n = 20$, both measured by SEM) (Fig. 3). Results for surface roughness, peak density, wettability and slipperiness of 13 formulated paints are shown in Table 3. The full set of data (45 paints) is given in Table S 1. Fig. 5A shows surface slipperiness as a function of PVC.

For the overall set of paints (1–45, Table S 1), the slipperiness for ants greatly increased with the PVC (Table 4, Spearman's rank test $r_s = 0.59$, $n = 45$, $P < 0.001$). The slipperiness increased strongly with the PVC for the paints containing only $CaCO_3$ (paints 10–18, $r_s = 0.80$, $n = 9$, $P = 0.010$), unlike TiO_2-paints (paints 1–9, $r_s = -0.62$, $n = 9$, $P = 0.074$). For some paints containing only TiO_2 (paints 4–6, Table 3), the reverse trend was observed: the higher the PVC, the lower the slipperiness. Unlike other coatings, TiO_2 paints tend to form cracks despite the presence of coalescent. This is likely due to the fact that TiO_2-only paints are further above their CPVC at PVCs 60 and 70 than the $CaCO_3$-only paints (54% vs. 63%). The number of cracks was found to increase with the PVC under SEM, as the amount of polymer binder is reduced. These cracks most likely provide good grip to insect claws: claw interlocking with surface asperities is possible if the asperity size is larger than the claw tip radius [41,50], which is for *A. cephalotes* 5.0 ± 1.7 μm ($n = 31$). The cracks present larger dimensions (at least 10 μm in width) and one can imagine that once the claws get into contact with the paint, the cracks may expand due to the coating stiffness. Image examples of the cracks are given in Figure S 1 (A and B, Supplementary material).

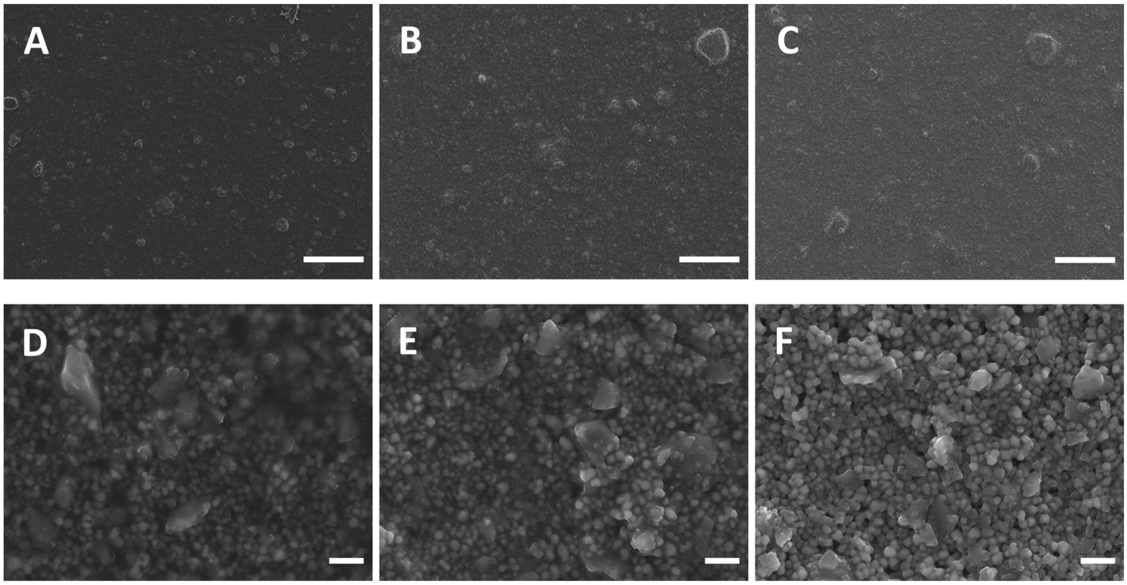

Fig. 4. SEM images of 30 wt% TiO_2, 20 wt% $CaCO_3$ paint surfaces with varying PVC: (A, D) PVC 50, (B, E) PVC 60 and (C, F) PVC 70. Paints shown in (B, E) and (C, F) are formulated above their CPVC. Scale bars: (A–C) 100 μm and (D–F) 1 μm.

The paints containing only $CaCO_3$ were found to be more slippery for ants than TiO_2-only paints, at PVC 70 in particular (Table S 1). Neither the amounts of TiO_2 nor $CaCO_3$ were found to significantly influence slipperiness (slipperiness × TiO_2: r_s = -0.12, n = 45, P = 0.449; slipperiness × $CaCO_3$: r_s = 0.09, n = 45, P = 0.572). Although non-significant at α = 0.05, the slipperiness results obtained in the PVC 70 paint series may suggest an impact of the CaCO3 amount on the slipperiness (r_s = -0.49, n = 27, P = 0.064, Table S 1). This suggests that both particle size and shape influence insect attachment to surfaces. Optimum paint formulations that maximise the slipperiness for *A. cephalotes* ants included 20 wt% TiO_2 and 20 wt% $CaCO_3$. In these conditions, it is important to note that our surfaces achieved high slipperiness on vertical paints (90% of ants fallen, PVC 70), while only 44% cockroaches could not escape 60° tilted surfaces coated with insect-repellent polymers prepared by Graf et al. [69].

Based on our observations, we further investigated three hypotheses to explain why both high PVC and $CaCO_3$ paints are slippery to ants: (1) surface roughness, (2) surface wettability, and (3) particle detachment. It should be noted that because of the similar design and performance of insect adhesive pads, the observed slipperiness trends may possibly apply to many other insects [36,70,87].

3.2. Effect of surface roughness

The surface roughness of the paint coatings is based on both the presence of large particles at the surface and the formation of clusters formed by self-aggregation of extender and pigment [92–94]. It is worth mentioning that small calcium carbonate grades can reduce TiO_2 self-aggregation, which is referred to as the spacing effect of $CaCO_3$ [95], and can be driven by the opposite surface zeta potentials between TiO_2 and $CaCO_3$ [96]. However, our SDS-stabilised TiO_2 and $CaCO_3$ particles both displayed negative zeta potential values (data not shown), indicating that the formation of aggregates should be hindered by electrostatic repulsion [92].

Fig. 5B shows that the R_a values ranged from 1 μm to 5.5 μm, the median values slightly increased with the PVC, with similar data distributions between the three PVC series. Paints 11, 14 and 17 exhibited large roughness values (R_a > 10 μm, Table 3) and are hence not shown in Fig. 5B for more clarity. These are 60% PVC CaCO3-only paints which reached their CPVC at PVC 60, leading to very rough surfaces [91]. Even when removing these outliers, R_a did not significantly increased with PVC at α = 0.05, but it is commonly accepted that paint formulated with increasing PVC lead to rougher coatings (r_s = 0.30, n

Table 3
Composition, CPVC, PVC, surface roughness (R_a), peak density, wettability and slipperiness values of 13 custom-made waterborne paints applied on metal sheets. The CPVC was approximated from eq. (3). Both R_a and peak density were measured *via* optical profilometry. The slipperiness to *A. cephalotes* ants refers to the percentage of unsuccessful ants in climbing tests. The values are expressed as mean ± standard deviation (SD). See section Materials and methods for further explanations. The full set of paints is described inTable S 1 (Supplementary material).

Paint	[TiO_2] (wt %)	[$CaCO_3$] (wt %)	Approximate CPVC (%)	PVC (%)	R_a (μm) (n = 6)	Peak density (peaks/mm^2) (n = 6)	Water contact angle (°) (n = 4)	Slipperiness (%) (n = 20)
2	10	0	54	60	2.7 ± 0.2	339 ± 101	98 ± 3	90 ± 10
4	20	0	54	50	2.2 ± 0.7	374 ± 134	79 ± 8	20 ± 10
5	20	0	54	60	1.9 ± 0.4	42 ± 3	102 ± 8	10 ± 10
6	20	0	54	70	5.3 ± 1.0	20 ± 6	86 ± 5	0 ± 10
8	30	0	54	60	2.6 ± 0.3	30 ± 15	100 ± 3	40 ± 10
11	0	6.6	63	60	26.7 ± 4.5	304 ± 51	62 ± 3	30 ± 10
14	0	13	63	60	13.0 ± 4.6	394 ± 59	73 ± 1	30 ± 10
17	0	20	63	60	30.0 ± 10.2	49 ± 12	71 ± 1	20 ± 20
39	30	6.6	56	70	1.3 ± 0.4	299 ± 136	86 ± 5	87 ± 12
42	30	13	58	70	4.8 ± 0.1	1156 ± 41	94 ± 1	90 ± 10
43	30	20	59	50	4.8 ± 0.1	1136 ± 33	53 ± 2	10 ± 10
44	30	20	59	60	4.9 ± 0.1	1110 ± 88	66 ± 1	10 ± 10
45	30	20	59	70	4.6 ± 0.1	1140 ± 46	89 ± 3	90 ± 10

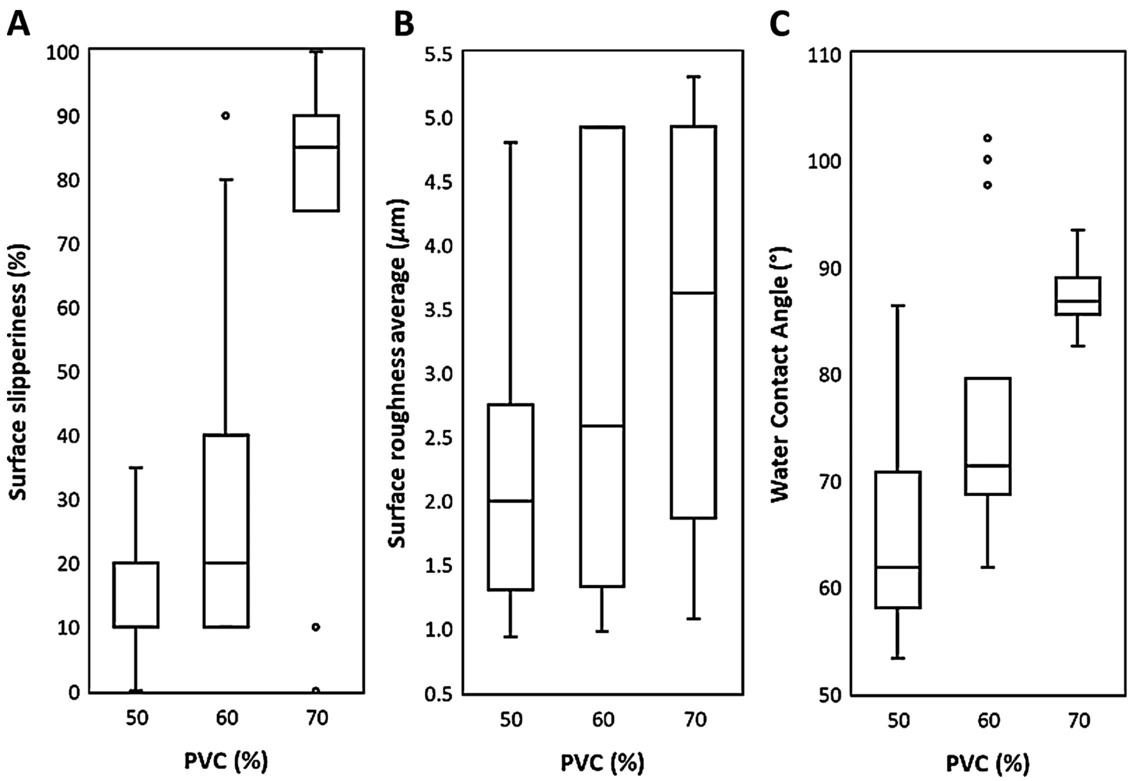

Fig. 5. Boxplots showing (A) surface slipperiness (percentage of unsuccessful ants in climbing tests), (B) surface roughness average (R_a) and (C) water contact angle measured for the full set of paints formulated at different PVC values. In (B), three outliers (R_a > 10 μm) were not shown for more clarity. Centre lines and boxes represent the median within the 25th and 75th percentiles, whiskers show the 10th and 90th percentiles and circles indicate outliers.

= 42, P = 0.053) [80,81,92].

It has been suggested that insect attachment forces are decreased on micro-rough surfaces (0.3-1.0 μm asperity size) [50,51], as well as paints [70], because the small asperities reduce the contact area for the adhesive pads but do not allow the claws to interlock. Despite the wide range of slipperiness values (0–100% unsuccessful ants), we did not observe any effect of roughness average R_a on slipperiness (Fig. 6, r_s = 0.14, n = 45, P = 0.358), suggesting that other mechanisms explain the reduction in ant attachment to paint coatings. It has been shown in the literature that insect attachment forces to surfaces are minimised for asperity sizes in the submicron range (0.05-1 μm asperity size) [46,50–53,97]. We obtained a broad range of slipperiness values,

Table 4
: Correlation between test variables, correlation coefficient r_s and P-values obtained by Spearman's rank test for the following parameters: paint PVC, slipperiness, roughness average R_a, water contact angle and peak density for all paints, paints segregated by PVC and paint type. Only correlations with P-values indicating significant correlations (below α = 0.05) have been indicated for more clarity.

	Variable 1	Variable 2	Correlation coefficient r_s	P-value
All paints (n = 45)	PVC	Slipperiness	0.60	< 0.001
	PVC	Water contact angle	0.74	0
	Water contact angle	Slipperiness	0.54	< 0.001
	[$CaCO_3$]	Water contact angle	−0.37	0.011
	[$CaCO_3$]	Peak density	0.51	< 0.001
PVC 50 paints (n = 15)	[$CaCO_3$]	Water contact angle	0.71	0.003
	Peak density	Water contact angle	−0.65	0.008
	Water contact angle	Slipperiness	0.54	0.036
PVC 60 paints (n = 15)	[TiO_2]	R_a	−0.53	0.043
	[$CaCO_3$]	Water contact angle	−0.63	0.013
PVC 70 paints (n = 15)	[TiO_2]	Water contact angle	0.68	0.006
	[$CaCO_3$]	Peak density	0.58	0.025
TiO_2-only paints (n = 9)	PVC	R_a	0.86	0.003
	PVC	Peak density	−0.79	0.011
	Peak density	Slipperiness	0.67	0.050
$CaCO_3$-only paints (n = 9)	PVC	Slipperiness	0.80	0.010
	PVC	Water contact angle	0.85	0.003
	Water contact angle	Slipperiness	0.71	0.003
TiO_2/$CaCO_3$ paints (n = 27)	PVC	Slipperiness	0.89	0
	PVC	Water contact angle	0.90	0
	Water contact angle	Slipperiness	0.90	0
	R_a	Peak density	0.42	0.029

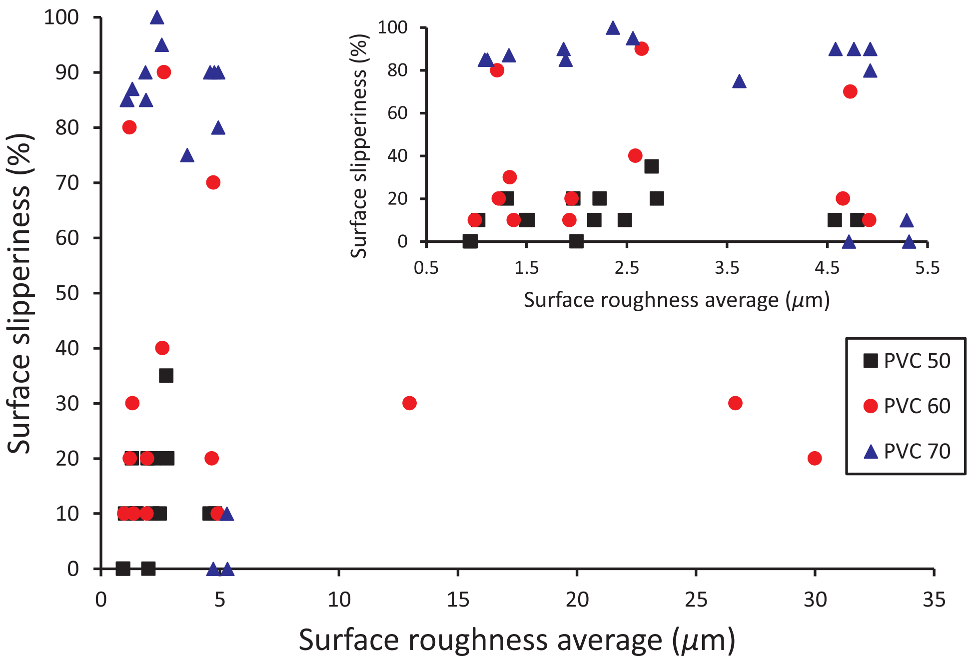

Fig. 6. Surface slipperiness (percentage of unsuccessful ants) of model paints formulated at different PVCs vs. surface roughness average R_a for PVCs 50, 60 and 70; inset: detail of 0.5-5.5 μm roughness. It can be seen that an effect of R_a on slipperiness cannot directly be concluded from this graph. Error bars are not included for more clarity.

despite our pigment particles being in the same size range as the surface asperities used in the various studies (ca. 300 nm TiO_2 and 1 μm $CaCO_3$ particles). However, the slipperiness of surfaces is not only based on roughness average R_a, but also on the lateral dimensions of surface roughness (e.g. asperity spacing and slope). Optical profilometry has a limited XY-resolution (ca. 500 nm) for capturing the lateral length scale of surface roughness. Measuring surface roughness *via* AFM proved difficult due to the large height differences of some coatings.

Defining peaks as any protruding regions greater than 5% of the largest asperity (relative to the midline), we measured the peak density by profilometry in 1 mm × 1 mm areas (Table S 1). 'Low' values (< 300 peaks/mm^2) were generally due to the formation of large aggregates at the surface. 'Large' values indicate that many narrow peaks were formed. Although there is no linear correlation between the peak density and the slipperiness (r_s = 0.15, n = 45, P = 0.327), the peak density seems to slightly influence the slipperiness for $CaCO_3$-only paints and $TiO_2/CaCO_3$ paints. For these two series, the slipperiness decreases until reaching the approximate threshold values of 200 and 600 peaks/mm^2, respectively (Figure S 2, Supplementary material, dashed lines), from which the slipperiness increases with the density. This suggests that 200 peaks/mm^2 and 600 peaks/mm^2 are the peak densities at which ants' adhesive pads can make full contact with the surface asperities for $CaCO_3$-only paints and $TiO_2/CaCO_3$ paints, respectively. We propose that the slipperiness in TiO_2-only paints is mainly driven by the cracks, and hence does not depend on the number of peaks.

One can imagine that rigid surface asperities may damage or destroy the smooth adhesive pad (arolium) of the ant, hence reducing contact between the pad and the substrate [98]. Wear damage would result in stiffening of the pad after several days. This cannot be readily observed by direct visual means as *A. cephalotes* ants possess retractable adhesive pads [89], and no apparent pad damage could be observed under SEM. Our results have not clearly demonstrated an influence of R_a on slipperiness; hence, other factors such as surface hydrophobicity or particle detachment must be considered.

3.3. Effect of surface wettability

As a high surface hydrophobicity or low surface energy of various surfaces has been found to affect attachment forces of beetles to some extent, we investigated the effect of the water contact angle on the slipperiness [45–48].

All water contact angles of the paint coatings were between 50° and 105°, with TiO_2- and $CaCO_3$-only paints displaying higher contact angles. The three outlier data points correspond to paints 2, 5, and 8 (Table 3), which are PVC 60 TiO_2-only paints reaching their CPVC and hence showing large contact angles [91]. The water contact angle greatly increased with the PVC (Table 4, r_s = 0.74, n = 45, P = 0).

Fig. 7 shows the effect of paint wettability on slipperiness for $TiO_2/CaCO_3$ paints. One can see in Table 4 that paint slipperiness was significantly correlated to both PVC (r_s = 0.59, n = 45, P < 0.001) and paint wettability (r_s = 0.54, n = 45, P < 0.001).

Fluid-mediated wet adhesion in insects occurs through van der Waals, capillary and viscous forces [30,39,40]. The biphasic fluid secreted by insects has been shown to decrease adhesion and friction forces on smooth surfaces, as well as increasing attachment forces on rough substrates by filling asperities [37,99]. The secretion is mainly oily and therefore wets most substrates [43], including rough surfaces [100]. The adhesive fluid's oily phase has been suggested to aid attachment on both hydrophilic and hydrophobic substrates [43,44,100].

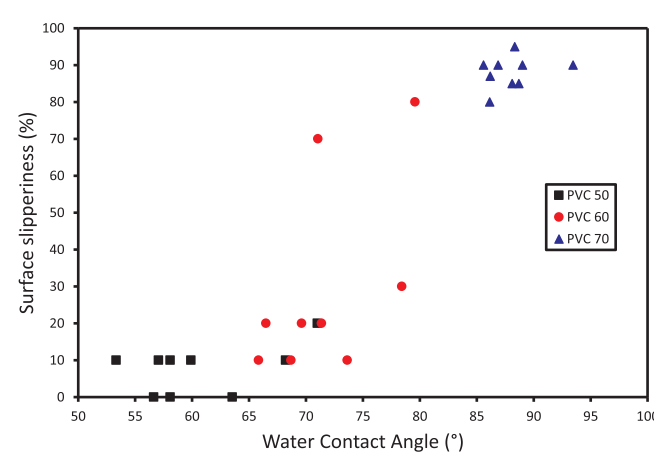

Fig. 7. Contact angle of water on paint surface vs. slipperiness (portion of unsuccessful ants) and PVC. One can see that both slipperiness and water contact angle increased with PVC. Data points corresponding to TiO_2- and $CaCO_3$-only paints and error bars were not included for more clarity.

However, the slipperiness to ants increased with a reduced wettability (for water) of the paint coatings. It is unlikely that this effect is based on insufficient wetting by the adhesive fluid; instead, slipperiness and water contact angle are both influenced by the PVC, rather than directly correlated.

An ANOVA test was performed to assess which parameters influenced the slipperiness the most. To this end, the slipperiness data were arcsine-transformed to achieve a homogeneous distribution of the variances of the residuals. To avoid artefacts resulting from the ordering of factors in unbalanced datasets, we conducted an ANOVA based on Type II sums of squares. By minimising the model to the most relevant parameters (PVC, R_a, contact angle and peak density), the minimal model contained several significant interactions that involved all the factors (Table S 2, Supplementary material). The parameters affecting significantly the slipperiness were the PVC ($F_{1,38} = 12.93$, $P < 0.001$), the peak density ($F_{1,38} = 5.22$, $P = 0.028$) and interactions between the parameters (interaction wettability × peak density, $F_{1,38} = 13.87$, $P < 0.001$; interaction Ra × PVC, $F_{1,38} = 17.21$, $P < 0.001$).

The explanatory variables of this analysis are correlated with each other, in particular WCA and PVC (Table 4). We conducted a Principal Component Regression (PCR) to decorrelate the explanatory factors. The explanatory variables could be reduced to three principal components (PCs) that explained 95% of the variation (Eq. (5), Supplementary material). Slipperiness depended most strongly on PC1, which was mainly associated with PVC and water contact angle (Table S 3).

3.4. Particle/aggregate detachment from the paint surfaces

As an alternative explanation as to why high PVC paints are slippery, we considered the hypothesis of detachment of particles from the paints. Particle detachment can lead to contamination of insect tarsal adhesive pads [62,101]. After climbing paint surfaces, the legs of *A. cephalotes* ants were removed and observed under the SEM (Fig. 8). We found that the arolium and hairs were contaminated by aggregates coming from the paint surfaces. In particular, the contamination level appeared to increase with the PVC. Quantification of the contaminating particles was challenging as individual particles could not always be distinguished due to the presence of polymer binder 'gluing' the particles together. From the SEM micrographs given in Fig. 8, we estimated that one pad detached approximately 51 and 203 particles from the PVC 60 and 70 paints containing 30% TiO_2, 20% $CaCO_3$, respectively. This confirms that particles detach more easily from paints with a higher PVC. Our results suggest that similarly to some pitcher plant surfaces, in which epicuticular wax crystals detach [56,57,60], aggregates detach from the paint surfaces and adhere to the tacky pads of leaf cutter ants. Particle detachment is based on the small amount of polymer, which results in incomplete wetting of the solid particles when paints are formulated above their CPVC.

We propose that the slipperiness is also based on insect pad contamination, leading to reduction or loss of contact area between the pad and the surface's irregularities.

The forces generated to detach pigment and extender particles should be stronger than the hydrogen and electrostatic bonding between the polymer binder and the particles [102] and should also fracture the polymer adsorbed onto the surface of particles [103]. Anyon et al. suggested the adhesive force necessary for particles to contaminate arolia increases with both the particle's radius and the surface tension of the insect's adhesive secretion [101,104]. When contaminating particles are present on insect pads, they can be removed through self-cleaning, which, during locomotion, occurs when the arolium is subject to shear forces that help remove the fouling particles [103,105]. The insects' adhesive fluid was found to aid the process by filling the gaps between the particles, then increasing the contact area and hence, the adhesion and friction forces [106]. The self-cleaning time depends on the insect species and hence, pad type, as well as the size, nature and surface energy of the fouling particles [106–108]. In beetles, 1 μm and larger than 45 μm fouling particles were found to be removed in a few steps, unlike 10-20 μm particles, which fit in between the hairs of the beetles' pads and hence needed more steps to be removed [105,107,108].

To further test our hypothesis that paint surfaces are slippery through the detachment of particles, we allowed ants that had been climbed on 30 wt% TiO_2, 20 wt% $CaCO_3$ paints (43–45, Table 3) to climb on clean glass using a simple double-vial set-up (Fig. 9). At PVC 50, the ants could climb up the glass immediately after falling off from the surface of the painted vial, while they needed 5 min and 55 min to climb up glass again for the PVC 60 and 70 paints, respectively. These results support the argument that slipperiness is mainly due to pad contamination. They also allow us to estimate the self-cleaning time of *A. cephalotes* ants, which corresponds to the time needed to remove contaminating particles from their pads [106,108].

Paints containing only $CaCO_3$ were found to show greater slipperiness than TiO_2-only paints, at PVC 70 in particular, as shown in Table S 1. We tentatively explain this by an easier detachment of $CaCO_3$ particles from the paint surface, as $CaCO_3$ particles are larger than TiO_2 particles (ca. 1 μm vs. 300 nm) and as their irregular shape (platelet vs. spherical particles) prevents strong attachment. Liquid calcium carbonate-based dispersions have already been shown to be efficient against termites to prevent wood infestation [24]. Although one could expect that some pigment particles may segregate to the bottom of the surface in the absence of thickener [93,94], SEM micrographs show that both types of particle were present at the surface (Fig. 4).

The TiO_2 and $CaCO_3$ particles had similar oil absorption values (19 and 20 g per 100 g, respectively), which indicate how much binder is needed to fully cover the particles. Oil absorption was therefore not considered a significant parameter explaining why the $CaCO_3$ detached more easily than TiO_2 particles. It is possible that either insect pads have greater affinity for $CaCO_3$ particles, or that TiO_2 particles are more tightly bound to the acrylic polymer film. The latter hypothesis should be tested in further work using polymer-pigment adsorption isotherms [102].

It is noteworthy to mention that the paints, depending on the TiO_2/$CaCO_3$ combination, present slight variations in their CPVC (54–63%, Table S 1). For smaller CPVC values (e.g. TiO_2-only paints), it is expected that the particles should detach more easily at PVC 60 and 70, as these PVC values are well above the CPVC. However, this was generally not observed, in particular for the TiO_2-only paints which showed low slipperiness values, and the optimised formulations containing 20 wt% TiO_2, 20 wt% $CaCO_3$, *i.e.* presenting an approximate CPVC value of 59%.

The effect of the type, size and shape of the extender particles on the paint slipperiness will be explored in further studies. It is expected that particles larger than the spacing between the two claws, approximately 69 ± 11 μm ($n = 25$) for *A. cephalotes* as measured by SEM, cannot contaminate the ants' arolia [101]. For particles showing wide size distributions, only the smaller particles could foul arolia. Contamination may be enhanced by the capillary adhesion between the ants' fluid and the particles, similar to that observed between polymer binder and pigment particles [102].

3.5. Long-term slipperiness and paint durability

Since particles detach from the paints, it is important to assess both the mechanical stability, or durability, and the long-term slipperiness of the coatings. The scrub resistance test simulates how paints cope with wear over time. Coatings were rubbed with a scrubbing pad and an abrasive surfactant solution (2.5 g/L sodium dodecylbenzenesulfonate) for either 200 or 2000 cycles at a speed of 36 cycles/min by applying a force of 2.4 N.

We randomly selected three PVC 70 paints from our sample set, which were scrubbed to 200 cycles (Table 5). All coatings showed good durability, in particular paint 33 (20 wt% TiO_2, 13 wt% $CaCO_3$), which

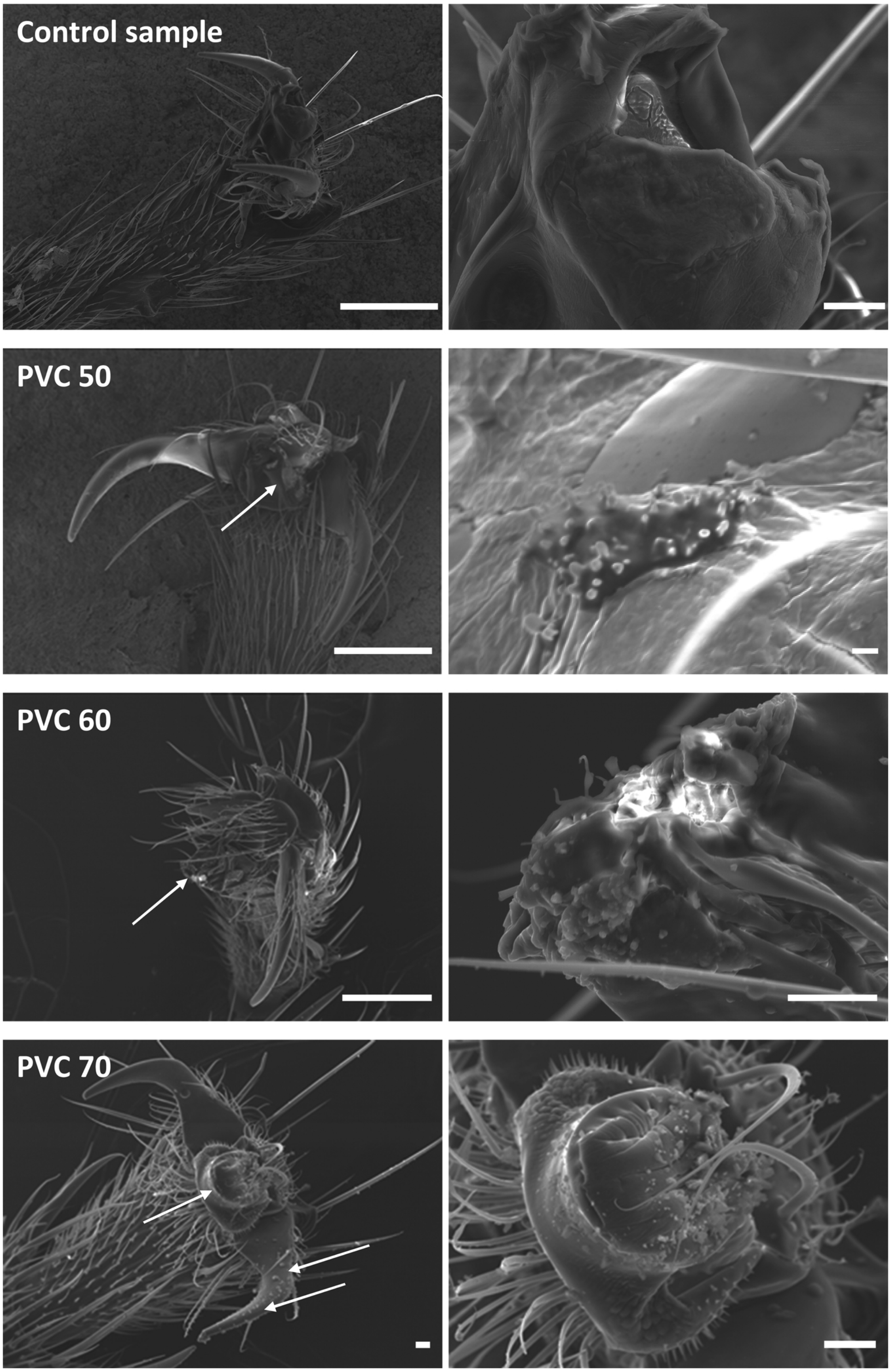

Fig. 8. SEM images of *A. cephalotes* ant tarsi contamination after climbing 30 wt% TiO_2, 20 wt% $CaCO_3$ paint surfaces formulated at PVC 50, 60 and 70. Control sample: ants which did not climb on paint, no contaminants could be observed. Scale bars: 100 μm (left) and 10 μm (right). PVC 50: only a few contaminating particles could be observed on the arolium; scale bars: 100 μm (left) and 1 μm (right). PVC 60: the arolium tip was fouled by paint particles. Scale bars: 100 μm (left) and 10 μm (right). PVC 70: the arolium and claws were heavily contaminated by particles, mostly $CaCO_3$. Arrows show contaminating particles. Scale bars: 10 μm (left) and 10 μm (right).

was further scrubbed for 2000 cycles. Ant climbing tests were performed on these scrubbed panels.

After scrubbing (200 and 2000 cycles), high slipperiness values were observed for the three coatings. We found that after being scrubbed, the paint surfaces exposed more loose particles at their top surface, and one can clearly see that the ants' pads were heavily fouled (Fig. 10), in particular with $CaCO_3$ particles, supporting the earlier assumption that either their pads present greater affinity for $CaCO_3$ than TiO_2 particles, or that TiO_2 particles are more tightly bound to the coating. The surface roughness values suggest that ants used their claws to cling to surface asperities, but particles were also found on their arolia. This further suggests that particle detachment is the main mechanism which prevents leaf cutting ant workers from climbing on PVC 70 paints.

To measure the long-term slipperiness of the paints, we placed paints of the 30 wt% TiO_2 series, with varying $CaCO_3$ concentrations (paints 39, 42 and 45, Table 3) on the walls at the bottom of the cage containing a large *A. cephalotes* colony so that the ants had direct access to the panels, and recorded the slipperiness over five months. Fig. 11 illustrates that the slipperiness gradually decreased over time, and that surfaces were more slippery when the paints contained more $CaCO_3$. After five months, the 30 wt% TiO_2, 20 wt% $CaCO_3$ paint still displayed

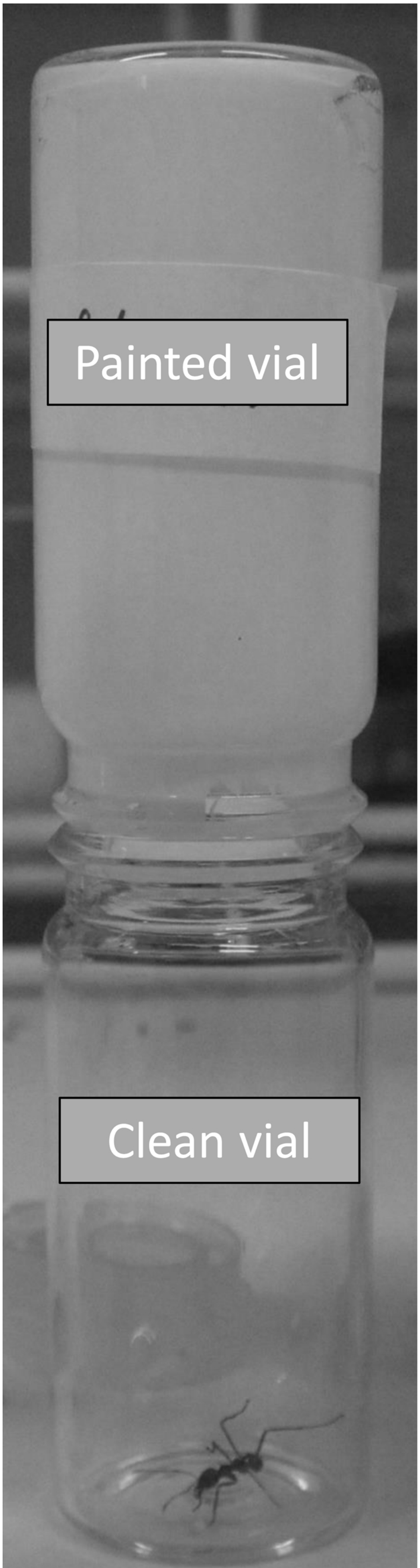

Fig. 9. Double-vial set-up to test the particle detachment hypothesis after contamination of feet of *A. cephalotes* ants: the top vial was painted with test paint and the bottom vial was clean glass.

approximately 70% slipperiness (significant difference between t = 0 and t = 5 months, paired *t*-test, $T_2 = 5.29$, $P = 0.034$).

Interestingly, the slipperiness first gradually decreased over the first two months of testing, and then reached a plateau at about 33%, 60% and 70% slipperiness for paints containing 6.6 wt%, 13 wt% and 20 wt % $CaCO_3$, respectively. These results suggest that *A. cephalotes* ants removed most of the loose, detachable particles within the first two months and thereafter, their attachment was mainly reduced due to the surface asperities. As particles still detached from all tested scrubbed paint panels to the ant's arolia, the particle detachment forces produced by the ants' feet may be at least as strong as those in the scrub test.

A similar effect has been proposed for *N. alata* pitcher plants, where the slippery surface is composed of two layers of epicuticular wax crystals [56,57,60]. The crystals of the upper layer detach upon contact with insect tarsi and do not regenerate [58]. Mechanical removal of the whole upper layer using dental wax lift-off left behind a rough bottom layer that still reduced insect adhesion [53,56]. Assuming that the upper layer also becomes fully removed by insect pads, the surface roughness of the bottom layer alone could reduce insect attachment. However, it is unclear to what extent the upper layer is removed by insect feet under natural conditions, and if the remaining surface is comparable to that obtained *via* experimental lift-off. The SEM of ant pads after climbing the paints, after being placed for five months in the colony cage, showed that there were no more particles attached to their arolia (Figure S 3, Supplementary material). The profilometry measurements of the paint panels showed the roughness average R_a had dramatically increased due to pigment removal, by 330% on average, and was significantly different for paints 39 (Mann-Whitney $U_{10,6} = 0$, $P = 0.001$) and 45 ($U_{10,6} = 0$, $P = 0.001$), but not for 42 ($U_{10,6} = 18$, $P = 0.211$) between t = 0 months and t = 5 months (Table S 4, Supplementary material).

It is important to note that the number of climbing ants decreased over time as a result of behavioural adaptations (A.F., personal observation). In real-life conditions, it is assumed that after a few climbing trials, insects would forage or nest elsewhere [88,109]. From our results, we estimate that ten ants try to climb the paints per minute, *i.e.* about 14,000 insects per day assuming constant activity. From ant pads analysed by SEM after climbing paint 45 (Fig. 8, PVC 70), about 200 particles were removed by one pad, which is low compared to the approximate number of 2.9×10^{12} particles contained in the paint film (Eq. (9) Supplementary material). Based on their shape, most fouling particles seemed to be $CaCO_3$ particles. An estimate of the removed particle weight was not possible as the ants had left trail secretions on the panels, possibly to mark their territory [110]. Assuming that 14,000 ants removed 200 particles per pad daily for two months, then about a billion particles would be removed, *i.e.* about 3.4% of the total amount of particles contained in the paint film. Considering these rough orders of magnitude, this suggests that the fraction of loose pigment and extender particles in the coating is relatively low as they were removed in about two months by the ants.

It is known that high PVC paints generally present low mechanical stability and low gloss, in particular when formulated above their CPVC [93]. However, our model paints showed good durability (Table 5), likely due to the absence of hydrophilic compounds, which tend to decrease the durability (scrub resistance) of coatings. Our $CaCO_3$-only and $TiO_2/CaCO_3$ PVC 70 paints showed a good balance between mechanical properties and long-term, high slipperiness. However, it must be noted that these coatings are unlikely to withstand outdoor conditions, e.g. weathering or rain, due to the absence of adequate additives.

Table 5
: Slipperiness and roughness average (R_a) comparison of scrubs panels before and after scrubbing the paints (200 or 2000 cycles). The values are expressed as mean ± standard deviation (SD).

Paint	[TiO_2] (wt %)	[$CaCO_3$] (wt %)	Number of cycles	Scrub resistance (mg/ cm^2) ($n = 2$)	Slipperiness before scrubs (%) ($n = 20$)	Slipperiness after scrubs (%) ($n = 20$)	R_a before scrubs (μm) ($n = 6$)	R_a after scrubs (μm) ($n = 6$)
24	10	13	200	0.38 ± 0.08	90 ± 5	100 ± 10	6.0 ± 3.4	9.4 ± 7.2
39	30	6.6	200	0.23 ± 0.05	87 ± 12	100 ± 10	5.9 ± 4.3	6.8 ± 4.3
33	20	13	2000	0.75 ± 0.17	85 ± 5	100 ± 10	4.4 ± 3.5	11.8 ± 6.3

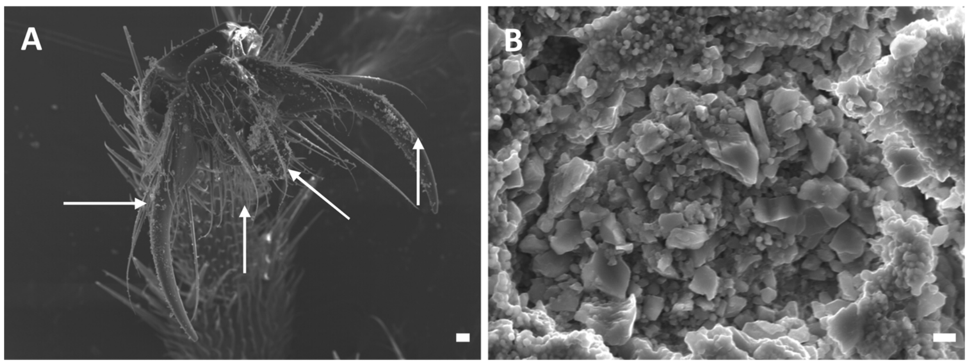

Fig. 10. SEM images of (A) contaminated *A. cephalotes* tarsus after climbing a scrubbed paint panel. Arrows show contaminating particles. (B) exposed "craters" rich in loose particles after the coating was scrubbed for 2000 cycles. Scale bars: (A) 10 μm and (B) 1 μm.

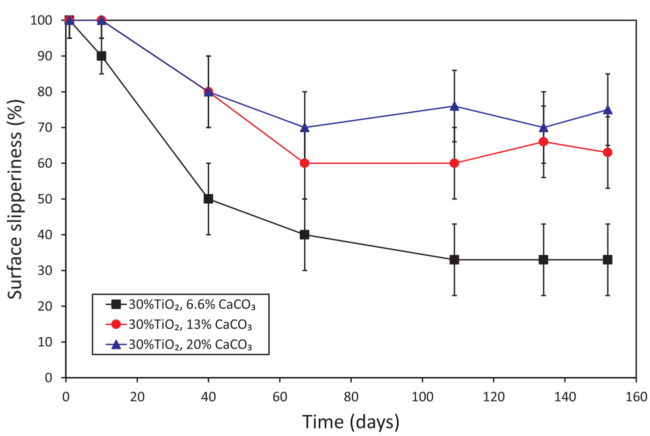

Fig. 11. Long-term slipperiness test: slipperiness (portion of unsuccessful ants) measured as a function of time during 5 months by leaving the painted panels (30% TiO_2, variable concentration of $CaCO_3$) in the *A. cephalotes* colony's rearing. A slipperiness plateau was reached within ca. 2 months for the three paints, which suggests that thereafter, insect attachment forces were reduced through surface roughness.

4. Conclusions

Insect-slippery model paints were prepared using an acrylic polymer binder, 300 nm TiO_2 and 1 μm $CaCO_3$ particles. Our findings show that ant workers (*A. cephalotes*) could not adhere to the vertical surfaces of some paints mainly due to particle detachment, in combination with surface roughness. A long-term insect exposure experiment showed that even after detachment of most loose particles, the paints remained slippery for insects, likely due to their surface roughness. Insect attachment to paint surfaces was mainly related to the following paint formulation parameters:

1 Paint PVC (Pigment Volume Concentration): when above the Critical Pigment Volume Concentration (CPVC), loose particles will detach from the coating and adhere to ant pads, leading to a loss of contact.
2 The type, dimensions and shape of solid particles: CaCO3 particles were found to detach more easily from the paint than TiO2 particles, possibly due to their larger size (ca. 1 μm vs. 300 nm, Fig. 3) and shape (platelet vs. spherical) which may facilitate interlocking of claws and pads. Indeed, high PVC TiO2-only paints were not slippery. Paints containing 20 wt% $CaCO_3$ showed the best combination of slipperiness and mechanical (scrub) resistance.

The stiffness and yield strength of the coatings has not been tested here but may be important, as insect claws or spines can dig into soft substrates to get a grip [111]. The influence of the latex type (chemistry, particle diameter and temperature properties) as well as the extender (chemistry, size and geometry) will be further investigated. Finally, it will be important to verify our findings with tests on other insect species. Because of the similar effects of slippery substrates on insect adhesive pads [36,70,87], the observed trends may apply to all climbing insects.

Acknowledgement

A.F. wishes to thank Ann Robinson and John Jennings (AkzoNobel, UK) for their assistance in microscopy, as well as John Steele and Bogdan Ibanescu (AkzoNobel, UK) for their support with statistics. Victor Kang and Caroline Grannemann (University of Cambridge, UK) are acknowledged for their acquisition of the long-term slipperiness data. This work is supported by the European Union through the Horizon 2020 project BioSmart Trainee "Training in Bio-Inspired Design of Smart Adhesive Materials" (Grant agreement no: 642861).

Appendix A. Supplementary data

Supplementary material related to this article can be found, in the online version, at doi:https://doi.org/10.1016/j.porgcoat.2019.06.004.

References

[1] E.-C. Oerke, Crop losses to pests, J. Agric. Sci. 144 (2006) 31–43, https://doi.org/10.1017/S0021859605005708.
[2] B.M. Greenwood, D.A. Fidock, D.E. Kyle, S.H.I.I. Kappe, P.L. Alonso, F.H. Collins, P.E. Duffy, Malaria: progress, perils, and prospects for eradication, J. Clin. Invest. 118 (2008) 1266–1276, https://doi.org/10.1172/JCI33996.

[3] G.S. Dhaliwal, V. Jindal, A.K. Dhawan, Insect pest problems and crop losses: changing trends, Indian J. Ecol. 37 (2010) 1–7.
[4] C.Y. Lee, Tropical household ants: pest status, species diversity, foraging behavior and baiting studies, Proc. Fourth Int. Conf. Urban Pests. (2002) 3–18.
[5] X. Bonnefoy, H. Kampen, K. Sweene, Public Health Significance of Urban Pests, World Health Organization, Copenhagen, 2008.
[6] N.-Y. Su, R.H. Scheffrahn, Termites as pests of buildings, Termit. Evol. Soc. Symbioses, Ecol. Springer Netherlands, Dordrecht, 2000, pp. 437–453, https://doi.org/10.1007/978-94-017-3223-9_20.
[7] A. Ghaly, S. Edwards, Termite Damage to Buildings: Nature of Attacks and Preventive Construction Methods, Am. J. Eng. Appl. Sci. 4 (2011) 187–200, https://doi.org/10.3844/ajeassp.2011.187.200.
[8] G.K. Mahapatro, D. Chatterjee, Termites as structural pest: status in indian scenario, Proc. Acad. Sci. India Sect. B 88 (2018) 977–994, https://doi.org/10.1007/s40011-016-0837-5.
[9] T. Birkemoe, Structural infestations of ants (Hymenoptera, Formicidae) in southern Norway, Nor. J. Entomol. (1999) 49 (2002) 139–142.
[10] D.H. Oi, K.M. Vail, D.F. Williams, D.N. Bieman, Indoor and outdoor foraging locations of pharaoh ants (Hymenoptera: formicidae) and control strategies using bait stations, Florida Entomol. 77 (1994) 85, https://doi.org/10.2307/3495874.
[11] M. Verma, S. Sharma, R. Prasad, Biological alternatives for termite control: a review, Int. Biodeterior. Biodegradation 63 (2009) 959–972, https://doi.org/10.1016/j.ibiod.2009.05.009.
[12] D. Pimentel, Environmental and economic costs of the application of pesticides primarily in the United States, Environ. Dev. Sustain. 7 (2005) 229–252, https://doi.org/10.1007/s10668-005-7314-2.
[13] F. Sánchez-Bayo, K.A.G. Wyckhuys, Worldwide decline of the entomofauna: a review of its drivers, Biol. Conserv. 232 (2019) 8–27, https://doi.org/10.1016/j.biocon.2019.01.020.
[14] M. Lenz, B.L. Schafer, S. Runko, L. Glossop, The concrete slab as part of a termite barrier system: response of Australian subterranean termites to cracks of different width in concrete, Sociobiology 30 (1997) 103–118.
[15] UNEP, Finding Alternatives to Persistent Organic Pollutants (POPS) for Termite Management, (2000).
[16] S.K. Ghosh, Functional Coatings and Microencapsulation: A General Perspective, Wiley-VCH Verlag GmbH & Co. KGaA, Weinheim, FRG, 2006, https://doi.org/10.1002/3527608478.
[17] M. Whalon, G. Malloy, Insect Repellent Coatings, US5843215, 1998.
[18] M. Maia, S.J. Moore, Plant-based insect repellents: a review of their efficacy, development and testing, Malar. J. 10 (2011), https://doi.org/10.1186/1475-2875-10-S1-S11.
[19] G.R. Overman, Method for admixing plant essential oils to coatings for the purpose of repelling insects, US20090155394, 2009.
[20] P. Alexander, J.A. Kitchener, H.V.A.A. Briscoe, Inert dust insecticides: part I. Mechanism of action, Ann. Appl. Biol. 31 (1944) 143–149, https://doi.org/10.1111/j.1744-7348.1944.tb06225.x.
[21] D.M. Glenn, G.J. Puterka, Particle films: a new technology for agriculture, Hortic. Rev. (Am. Soc. Hortic. Sci), John Wiley & Sons, Inc., 2010, pp. 1–44, https://doi.org/10.1002/9780470650882 ch1..
[22] C.G. Athanassiou, F.H. Arthur, Bacterial insecticides and inert materials, Recent Adv. Stored Prod. Prot. Springer, Berlin, Heidelberg, 2018, pp. 83–98, https://doi.org/10.1007/978-3-662-56125-6.
[23] K. Shahzad, F. Manzoor, Nanoformulations and their mode of action in insects: a review of biological interactions, Drug Chem. Toxicol. (2019) 1–11, https://doi.org/10.1080/01480545.2018.1525393.
[24] M.W. Roomi, A.H. Shah, M. Anwarullah, M. Hussain, Studies on the control of subterranean termites by inorganic pesticides, Anzeiger Für Schädlingskd, Pflanzenschutz Umweltschutz. 63 (1990) 50–52, https://doi.org/10.1007/BF01903465.
[25] S.E. Donovan, P. Eggleton, W.E. Dubbin, M. Batchelder, L. Dibog, The effect of a soil-feeding termite, *Cubitermes fungifaber* (Isoptera: termitidae) on soil properties: termites may be an important source of soil microhabitat heterogeneity in tropical forests, Pedobiologia (Jena). 45 (2001) 1–11, https://doi.org/10.1078/0031-4056-00063.
[26] H.I.J. Black, M.J.N. Okwakol, Agricultural intensification, soil biodiversity and agroecosystem function in the tropics: the role of termites, Agric., Ecosyst. Environ., Appl. Soil Ecol. 6 (1997) 37–53, https://doi.org/10.1016/S0929-1393(96)00153-9.
[27] T.Z. Dawes, Reestablishment of ecological functioning by mulching and termite invasion in a degraded soil in an Australian savanna, Soil Biol. Biochem. 42 (2010) 1825–1834, https://doi.org/10.1016/j.soilbio.2010.06.023.
[28] B. Hölldobler, E.O.O. Wilson, The Ants, Harvard University Press, 1990.
[29] S.N. Gorb, Attachment Devices of Insect Cuticle, Kluwer Academic Publishers, Dordrecht, 2002, https://doi.org/10.1007/0-306-47515-4.
[30] S.N. Gorb, Biological and biologically inspired attachment systems, Springer Handb. Nanotechnol. Springer Berlin Heidelberg, Berlin, Heidelberg, 2010, pp. 1525–1551, https://doi.org/10.1007/978-3-642-02525-9_43.
[31] T. Endlein, W. Federle, On heels and toes: how ants climb with adhesive pads and tarsal friction hair arrays, PLoS One 10 (2015) e0141269, , https://doi.org/10.1371/journal.pone.0141269.
[32] J.H. Dirks, Physical principles of fluid-mediated insect attachment - Shouldn't insects slip? Beilstein J. Nanotechnol. 5 (2014) 1160–1166, https://doi.org/10.3762/bjnano.5.127.
[33] J.M.R. Bullock, W. Federle, Division of labour and sex differences between fibrillar, tarsal adhesive pads in beetles: effective elastic modulus and attachment performance, J. Exp. Biol. 212 (2009) 1876–1888, https://doi.org/10.1242/jeb.030551.
[34] D. Gladun, S.N. Gorb, L.I. Frantsevich, Alternative tasks of the insect arolium with Special reference to hymenoptera, Funct. Surfaces Biol. Springer, Dordrecht, 2009, pp. 67–103, https://doi.org/10.1007/978-1-4020-6695-5_4.
[35] M.W.J. Crosland, N.-Y. Su, R.H. Scheffrahn, Arolia in termites (Isoptera): functional significance and evolutionary loss, Insectes Soc. 52 (2005) 63–66, https://doi.org/10.1007/s00040-004-0779-4.
[36] J.M.R. Bullock, P. Drechsler, W. Federle, Comparison of smooth and hairy attachment pads in insects: friction, adhesion and mechanisms for direction-dependence, J. Exp. Biol. 211 (2008) 3333–3343, https://doi.org/10.1242/jeb.020941.
[37] P. Drechsler, W. Federle, Biomechanics of smooth adhesive pads in insects: influence of tarsal secretion on attachment performance, J. Comp. Physiol. A 192 (2006) 1213–1222, https://doi.org/10.1007/s00359-006-0150-5.
[38] J.-H. Dirks, W. Federle, Fluid-based adhesion in insects - principles and challenges, Soft Matter 7 (2011) 11047, https://doi.org/10.1039/c1sm06269g.
[39] A.F.G. Dixon, P.C. Croghan, R.P. Gowing, The mechanism by which aphids adhere to smooth surfaces, J. Exp. Biol. 152 (1990) 243–253.
[40] N.E. Stork, Experimental analysis of adhesion of *Chrysolina polita* (Chrysomelidae: coleoptera) on a variety of surfaces, J. Exp. Biol. 88 (1980) 91–107, https://doi.org/10.1177/1094670505279702.
[41] Z. Dai, S.N. Gorb, U. Schwarz, Roughness-dependent friction force of the tarsal claw system in the beetle *Pachnoda marginata* (Coleoptera, Scarabaeidae), J. Exp. Biol. 205 (2002) 2479–2488.
[42] T. Endlein, W. Federle, Walking on smooth or rough ground: passive control of pretarsal attachment in ants, J. Comp. Physiol. A 194 (2008) 49–60, https://doi.org/10.1007/s00359-007-0287-x.
[43] J.-H. Dirks, C.J. Clemente, W. Federle, Insect tricks: two-phasic foot pad secretion prevents slipping, J. R. Soc. Interface 7 (2010) 587–593, https://doi.org/10.1098/rsif.2009.0308.
[44] S.N. Gorb, Smooth attachment devices in insects: functional morphology and biomechanics, Adv. In Insect Phys. (2007), pp. 81–115, https://doi.org/10.1016/S0065-2806(07)34002-2.
[45] C. Grohmann, A. Blankenstein, S. Koops, S.N. Gorb, Attachment of *Galerucella nymphaeae* (Coleoptera, Chrysomelidae) to surfaces with different surface energy, J. Exp. Biol. 217 (2014) 4213–4220, https://doi.org/10.1242/jeb.108902.
[46] M.W. England, T. Sato, M. Yagihashi, A. Hozumi, S.N. Gorb, E.V. Gorb, Surface roughness rather than surface chemistry essentially affects insect adhesion, Beilstein J. Nanotechnol. 7 (2016) 1471–1479, https://doi.org/10.3762/bjnano.7.139.
[47] B. Prüm, H.F. Bohn, R. Seidel, S. Rubach, T. Speck, Plant surfaces with cuticular folds and their replicas: influence of microstructuring and surface chemistry on the attachment of a leaf beetle, Acta Biomater. 9 (2013) 6360–6368, https://doi.org/10.1016/j.actbio.2013.01.030.
[48] E. Gorb, S. Gorb, Effects of surface topography and chemistry of *Rumex obtusifolius* leaves on the attachment of the beetle *Gastrophysa viridula*, Entomol. Exp. Appl. 130 (2009) 222–228, https://doi.org/10.1111/j.1570-7458.2008.00806.x.
[49] N. Hosoda, S.N. Gorb, Underwater locomotion in a terrestrial beetle: combination of surface de-wetting and capillary forces, Proc. R. Soc. B Biol. Sci. 279 (2012) 4236–4242, https://doi.org/10.1098/rspb.2012.1297.
[50] J.M.R. Bullock, W. Federle, The effect of surface roughness on claw and adhesive hair performance in the dock beetle Gastrophysa viridula, Insect Sci. 18 (2011) 298–304, https://doi.org/10.1111/j.1744-7917.2010.01369.x.
[51] D. Voigt, J.M. Schuppert, S. Dattinger, S.N. Gorb, Sexual dimorphism in the attachment ability of the Colorado potato beetle *Leptinotarsa decemlineata* (Coleoptera: chrysomelidae) to rough substrates, J. Insect Physiol. 54 (2008) 765–776, https://doi.org/10.1016/j.jinsphys.2008.02.006.
[52] W. Federle, T. Bruening, Ecology and biomechanics of slippery wax barriers and wax running in *Macaranga*-ant mutualisms, Ecol. Biomech. CRC Press, Boca Ratón, Florida, Florida, 2006, pp. 163–183, https://doi.org/10.1201/9781420001594.ch8.
[53] I. Scholz, M. Buckins, L. Dolge, T. Erlinghagen, A. Weth, F. Hischen, J. Mayer, S. Hoffmann, M. Riederer, M. Riedel, W. Baumgartner, Slippery surfaces of pitcher plants: *Nepenthes*wax crystals minimize insect attachment via microscopic surface roughness, J. Exp. Biol. 213 (2010) 1115–1125, https://doi.org/10.1242/jeb.035618.
[54] W. Barthlott, C. Neinhuis, Purity of the sacred lotus, or escape from contamination in biological surfaces, Planta 202 (1997) 1–8, https://doi.org/10.1007/s004250050096.
[55] A. Solga, Z. Cerman, B.F. Striffler, M. Spaeth, W. Barthlott, The dream of staying clean: lotus and biomimetic surfaces, Bioinspir. Biomim. 2 (2007) S126–S134, https://doi.org/10.1088/1748-3182/2/4/S02.
[56] E. Gorb, K. Haas, A. Henrich, S. Enders, N. Barbakadze, S. Gorb, Composite structure of the crystalline epicuticular wax layer of the slippery zone in the pitchers of the carnivorous plant *Nepenthes alata* and its effect on insect attachment, J. Exp. Biol. 208 (2005) 4651–4662, https://doi.org/10.1242/jeb.01939.
[57] K. Koch, B. Bhushan, W. Barthlott, Multifunctional plant surfaces and smart materials, Springer Handb. Nanotechnol. Springer, Würzburg, 2010, pp. 1399–1436, https://doi.org/10.1007/978-3-642-02525-9_41.
[58] E.V. Gorb, M.J. Baum, S.N. Gorb, Development and regeneration ability of the wax coverage in *Nepenthes alata* pitchers: a cryo-SEM approach, Sci. Rep. 3 (2013), https://doi.org/10.1038/srep03078.
[59] H.F. Bohn, W. Federle, Insect aquaplaning: *nepenthes* pitcher plants capture prey with the peristome, a fully wettable water-lubricated anisotropic surface, Proc. Natl. Acad. Sci. 101 (2004) 14138–14143, https://doi.org/10.1073/pnas.0405885101.

[60] L. Gaume, P. Perret, E. Gorb, S. Gorb, J.-J. Labat, N. Rowe, How do plant waxes cause flies to slide? Experimental tests of wax-based trapping mechanisms in three pitfall carnivorous plants, Arthropod Struct, Dev. 33 (2004) 103–111, https://doi.org/10.1016/j.asd.2003.11.005.
[61] E.V. Gorb, S.N. Gorb, Anti-adhesive effects of plant wax coverage on insect attachment, J. Exp. Bot. 68 (2017) 5323–5337, https://doi.org/10.1093/jxb/erx271.
[62] E.V. Gorb, S.N. Gorb, Attachment ability of the beetle *Chrysolina fastuosa* on various plant surfaces, Entomol. Exp. Appl. 105 (2002) 13–28, https://doi.org/10.1046/j.1570-7458.2002.01028.x.
[63] T.-S. Wong, S.H. Kang, S.K.Y. Tang, E.J. Smythe, B.D. Hatton, A. Grinthal, J. Aizenberg, Bioinspired self-repairing slippery surfaces with pressure-stable omniphobicity, Nature. 477 (2011) 443–447, https://doi.org/10.1038/nature10447.
[64] A.K. Epstein, T.-S. Wong, R.A. Belisle, E.M. Boggs, J. Aizenberg, Liquid-infused structured surfaces with exceptional anti-biofouling performance, Proc. Natl. Acad. Sci. 109 (2012) 13182–13187, https://doi.org/10.1073/pnas.1201973109.
[65] J. Aizenberg, M. Aizenberg, S.H. Kang, T.S. Wong, P. Kim, Lubricated slippery surfaces with high pressure stability, optical transparency, and self-healing characteristics, US9121307, 2015.
[66] M.J. Coady, M. Wood, G.Q. Wallace, K.E. Nielsen, A.-M. Kietzig, F. Lagugné-Labarthet, P.J. Ragogna, Icephobic behavior of UV-cured polymer networks incorporated into slippery lubricant-infused porous surfaces: improving SLIPS durability, ACS Appl. Mater. Interfaces 10 (2018) 2890–2896, https://doi.org/10.1021/acsami.7b14433.
[67] R.W. Bittner, K. Bica, H. Hoffmann, Fluorine-free, liquid-repellent surfaces made from ionic liquid-infused nanostructured silicon, Monatshefte Für Chemie - Chem. Mon. 148 (2017) 167–177, https://doi.org/10.1007/s00706-016-1888-2.
[68] Y. Zhou, A. Robinson, U. Steiner, W. Federle, Insect adhesion on rough surfaces: analysis of adhesive contact of smooth and hairy pads on transparent microstructured substrates, J. R. Soc. Interface 11 (2014) 20140499, https://doi.org/10.1098/rsif.2014.0499.
[69] C. Graf, A.B. Kesel, E.V. Gorb, S.N. Gorb, J.-H.H. Dirks, Investigating the efficiency of a bio-inspired insect repellent surface structure, Bioinspir. Biomim. 13 (2018) 56010, https://doi.org/10.1088/1748-3190/aad061.
[70] Y. Zhou, Insect Adhesion on Rough Surfaces and Properties of Insect Repellent Surfaces (PhD Thesis), University of Cambridge, Cambridge, 2015.
[71] S. Radinovsky, G.W. Krantz, The use of Fluon to prevent the escape of stored-product insects from glass containers, J. Econ. Entomol. 55 (1962) 815–816, https://doi.org/10.1093/jee/55.5.815.
[72] J. Chen, X. Wei, Coated containers with reduced concentrations of Fluon to prevent ant escape, J. Entomol. Sci. 42 (2007) 119–121, https://doi.org/10.18474/0749-8004-42.1.119.
[73] M.K. Hansen, M. Larsen, K.-H. Cohr, Waterborne paints: A review of their chemistry and toxicology and the results of determinations made during their use, Scand. J. Work Environ. Health 13 (1987) 473–485.
[74] I. de F.A.A. Mariz, I.S. Millichamp, J.C. de la Cal, J.R. Leiza, High performance water-borne paints with high volume solids based on bimodal latexes, Prog. Org. Coatings. 68 (2010) 225–233, https://doi.org/10.1016/j.porgcoat.2010.01.008.
[75] P.R. Sperry, B.S. Snyder, M.L. O'Dowd, P.M. Lesko, Role of water in particle deformation and compaction in latex film formation, Langmuir 10 (1994) 2619–2628, https://doi.org/10.1021/la00020a021.
[76] P.A.A. Steward, J. Hearn, M.C.C. Wilkinson, An overview of polymer latex film formation and properties, Adv. Colloid Interface Sci. 86 (2000) 195–267, https://doi.org/10.1016/S0001-8686(99)00037-8.
[77] W. Scholz, Paint additives, Surf. Coatings, Springer Science + Business Media, Dordrecht, 1993, pp. 539–580, https://doi.org/10.1007/978-94-011-1220-8_31.
[78] W.K. Asbeck, M. Van Loo, Critical pigment volume relationships, Ind. Eng. Chem. 41 (1949) 1470–1475, https://doi.org/10.1021/ie50475a042.
[79] B. Müller, U. Poth, Paint formulation, Coatings Formul. Vincentz, Hanover, 2010, pp. 60–74.
[80] G. del Rio, A. Rudin, Latex particle size and CPVC, Prog. Org. Coatings. 28 (1996) 259–270, https://doi.org/10.1016/0300-9440(95)00604-4.
[81] V. Alvarez, M. Paulis, Effect of acrylic binder type and calcium carbonate filler amount on the properties of paint-like blends, Prog. Org. Coatings. 112 (2017) 210–218, https://doi.org/10.1016/j.porgcoat.2017.07.023.
[82] T. Ding, E.S. Daniels, M.S. El-Aasser, A. Klein, Film formation from pigmented latex systems: mechanical and surface properties of ground calcium Carbonate/Functionalized poly (*n*-butyl methacrylate-*co*-*n*-butyl acrylate) latex blend films, J. Appl. Polym. Sci. 100 (2005) 4550–4560, https://doi.org/10.1002/app.22535.
[83] B. Daniels, Christian Leonard Gruber, High solids pigmented latex compositions, US20120234490A1, 2012.
[84] J. Davies, J.G.P.G.P. Binner, The role of ammonium polyacrylate in dispersing concentrated alumina suspensions, J. Eur. Ceram. Soc. 20 (2000) 1539–1553, https://doi.org/10.1016/S0955-2219(00)00012-1.
[85] S. Baklouti, M.R. Ben Romdhane, S. Boufi, C. Pagnoux, T. Chartier, J.F. Baumard, Effect of copolymer dispersant structure on the properties of alumina suspensions, J. Eur. Ceram. Soc. 23 (2003) 905–911, https://doi.org/10.1016/S0955-2219(02)00208-X.
[86] B. Lohmeijer, R. Balk, R. Baumstark, Preferred partitioning: the influence of coalescents on the build-up of mechanical properties in acrylic core–shell particles (I), J. Coatings Technol. Res. 9 (2012) 399–409, https://doi.org/10.1007/s11998-012-9396-8.
[87] U. Bauer, W. Federle, The insect-trapping rim of *Nepenthes* pitchers, Plant Signal. Behav. 4 (2009) 1019–1023, https://doi.org/10.4161/psb.4.11.9664.
[88] R. Dukas, Evolutionary biology of insect learning, Annu. Rev. Entomol. 53 (2008) 145–160, https://doi.org/10.1146/annurev.ento.53.103106.093343.
[89] W. Federle, E.L. Brainerd, T.A. McMahon, B. Holldobler, Biomechanics of the movable pretarsal adhesive organ in ants and bees, Proc. Natl. Acad. Sci. 98 (2001) 6215–6220, https://doi.org/10.1073/pnas.111139298.
[90] R: a Language and Environment for Statistical Computing, R Development Core Team, Vienna, Austria, 2018https://www.r-project.org/.
[91] J. Wang, H. Xu, D. Battocchi, G. Bierwagen, The determination of critical pigment volume concentration (CPVC) in organic coatings with fluorescence microscopy, Prog. Org. Coatings. 77 (2014) 2147–2154, https://doi.org/10.1016/j.porgcoat.2013.12.010.
[92] J. Tang, E.S. Daniels, V.L. Dimonie, A. Klein, M.S. El-Aasser, Influence of particle surface properties on film formation from precipitated calcium carbonate/latex blends, J. Appl. Polym. Sci. 86 (2002) 891–900, https://doi.org/10.1002/app.11000.
[93] F. Tiarks, T. Frechen, S. Kirsch, J. Leuninger, M. Melan, A. Pfau, F. Richter, B. Schuler, C.-L. Zhao, Formulation effects on the distribution of pigment particles in paints, Prog. Org. Coatings. 48 (2003) 140–152, https://doi.org/10.1016/S0300-9440(03)00095-X.
[94] S. Farrokhpay, G.E. Morris, D. Fornasiero, Titania pigment particles dispersion in water-based paint films, J. Coatings Technol. Res. 3 (2006) 275–283, https://doi.org/10.1007/s11998-006-0023-4.
[95] P.F. Dietz, Spacing for better effects, Eur. Coatings J. 49 (2003) 14–20.
[96] F. Karakaş, M.S.S. Çelik, Effect of quantity and size distribution of calcite filler on the quality of water borne paints, Prog. Org. Coatings. 74 (2012) 555–563, https://doi.org/10.1016/j.porgcoat.2012.02.002.
[97] E.V. Gorb, N. Hosoda, C. Miksch, S.N. Gorb, Slippery pores: anti-adhesive effect of nanoporous substrates on the beetle attachment system, J. R. Soc. Interface 7 (2010) 1571–1579, https://doi.org/10.1098/rsif.2010.0081.
[98] Y. Zhou, A. Robinson, C. Viney, W. Federle, Effect of shear forces and ageing on the compliance of adhesive pads in adult cockroaches, J. Exp. Biol. 218 (2015) 2775–2781, https://doi.org/10.1242/jeb.124362.
[99] O. Betz, M. Frenzel, M. Steiner, M. Vogt, M. Kleemeier, A. Hartwig, B. Sampalla, F. Rupp, M. Boley, C. Schmitt, Adhesion and friction of the smooth attachment system of the cockroach *Gromphadorhina portentosa* and the influence of the application of fluid adhesives, Biol. Open 6 (2017) 589–601, https://doi.org/10.1242/bio.024620.
[100] A.E. Kovalev, A.E. Filippov, S.N. Gorb, Insect wet steps: loss of fluid from insect feet adhering to a substrate, J. R. Soc. Interface 10 (2012), https://doi.org/10.1098/rsif.2012.0639 20120639–20120639.
[101] M.J. Anyon, M.J. Orchard, D.M.A. Buzza, S. Humphries, M.M. Kohonen, Effect of particulate contamination on adhesive ability and repellence in two species of ant (Hymenoptera; Formicidae), J. Exp. Biol. 215 (2012) 605–616, https://doi.org/10.1242/jeb.063578.
[102] S. Farrokhpay, G.E. Morris, D. Fornasiero, P. Self, Effects of chemical functional groups on the polymer adsorption behavior onto titania pigment particles, J. Colloid Interface Sci. 274 (2004) 33–40, https://doi.org/10.1016/j.jcis.2004.02.026.
[103] B.N.J. Persson, Biological adhesion for locomotion on rough surfaces: basic principles and a theorist's view, MRS Bull. 32 (2007) 486–490, https://doi.org/10.1557/mrs2007.82.
[104] H.-J. Butt, W.J.P. Barnes, A. del Campo, M. Kappl, F. Schönfeld, Capillary forces between soft, elastic spheres, Soft Matter 6 (2010) 5930–5936, https://doi.org/10.1039/c0sm00455c.
[105] C.J. Clemente, J.M.R. Bullock, A. Beale, W. Federle, Evidence for self-cleaning in fluid-based smooth and hairy adhesive systems of insects, J. Exp. Biol. 213 (2010) 635–642, https://doi.org/10.1242/jeb.038232.
[106] C.J. Clemente, W. Federle, Mechanisms of self-cleaning in fluid-based smooth adhesive pads of insects, Bioinspir. Biomim. 7 (2012) 46001, https://doi.org/10.1088/1748-3182/7/4/046001.
[107] G.J. Amador, T. Endlein, M. Sitti, Soiled adhesive pads shear clean by slipping: a robust self-cleaning mechanism in climbing beetles, J. R. Soc. Interface 14 (2017), https://doi.org/10.1098/rsif.2017.0134 20170134.
[108] M.J. Orchard, M. Kohonen, S. Humphries, The influence of surface energy on the self-cleaning of insect adhesive devices, J. Exp. Biol. 215 (2012) 279–286, https://doi.org/10.1242/jeb.063339.
[109] T. Tomioka, Insect repellent coating and industrial product using the same, US2006177472, 2006.
[110] K. Jaffé, M. Bazire-Benazét, P.E. Howse, An integumentary pheromone-secreting gland in *Atta* sp: territorial marking with a colonyspecific pheromone in *Atta cephalotes*, J. Insect Physiol. 25 (1979) 833–839, https://doi.org/10.1016/0022-1910(79)90086-6.
[111] H.H. Goetzke, J.G. Pattrick, W. Federle, Froghoppers jump from smooth plant surfaces by piercing them with sharp spines, Proc. Natl. Acad. Sci. 116 (2019) 3012–3017, https://doi.org/10.1073/pnas.1814183116.